Electrochemical Energy Reviews (2024) 7:10
https://doi.org/10.1007/s41918-024-00217-w

REVIEW ARTICLE

Emerging Atomically Precise Metal Nanoclusters and Ultrasmall Nanoparticles for Efficient Electrochemical Energy Catalysis: Synthesis Strategies and Surface/Interface Engineering

Mingjie Wu[1,2,3] · Fang Dong[3] · Yingkui Yang[1] · Xun Cui[1] · Xueqin Liu[1] · Yunhai Zhu[1] · Dongsheng Li[4] · Sasha Omanovic[2] · Shuhui Sun[3] · Gaixia Zhang[5]

Received: 12 September 2023 / Revised: 3 January 2024 / Accepted: 4 February 2024

Abstract

Atomically precise metal nanocluster and ultrasmall nanoparticle catalysts have garnered significant interest in electrocatalysis applications due to their unique geometric and electronic structures. As an intermediate state between single-atom catalysts (SACs) and nanoparticles in size, nanoclusters with specific low nuclearity provide designated metallic states with multiple atoms or surface sites for the adsorption and transformation of reactants/intermediates. The unique catalytic properties of nanoclusters offer a novel platform for designing effective and efficient electrocatalysts, potentially surpassing the SACs in certain catalytic reactions. This review summarizes and discusses the latest progress of nanoclusters and ultrasmall nanoparticles for various electrocatalysis applications, including oxygen reduction reaction (ORR), oxygen evolution reaction (OER), CO_2 reduction reaction (CO_2RR), nitrogen reduction reaction (NRR), hydrogen evolution reaction (HER), various chemicals oxidation reaction (COR), etc. Specifically, this review highlights surface/interface chemical modification strategies and structure-properties relationships, drawing from the atomic-level insights to determine electrocatalytic performance. Lastly, we present the challenges and opportunities associated with nanocluster or ultrasmall nanoparticle electrocatalysts.

Keywords Electrocatalysts · Nanoclusters · Ultrasmall nanoparticles · Surface · Interface engineering · Single-atom catalysts (SACs)

✉ Sasha Omanovic
sasha.omanovic@mcgill.ca

✉ Shuhui Sun
shuhui.sun@inrs.ca

✉ Gaixia Zhang
gaixia.zhang@etsmtl.ca

[1] State Key Laboratory of New Textile Materials and Advanced Processing Technologies, Wuhan Textile University, Wuhan 430200, Hubei, China

[2] Department of Chemical Engineering, McGill University, Montreal, QC H3A 0C5, Canada

[3] Institut National de la Recherche Scientifique (INRS), Centre Energie Materiaux Telecommunications, Varennes, QC J3X 1P7, Canada

[4] Key Laboratory of Inorganic Nonmetallic Crystalline and Energy Conversion Materials, China, College of Materials and Chemical Engineering, Three Gorges University, Yichang 443002, Jiangxi, China

[5] Department of Electrical Engineering, École de Technologie Supérieure (ÉTS), Montreal, QC H3C 1K3, Canada

1 Introduction

The increasing global industrialization and over-exploitation of fossil fuels have induced a major growing issue of global warming [1]. The severe environmental problems in the current society resulting from using traditional fossil fuels (unsustainable coal, petroleum, natural gas, etc.) raise new requirements for a high-efficiency energy supply. Exploiting sustainable and clean energy conversion and storage systems shows significant potential for achieving the industrial advantages of national strategic resources [2]. Electrochemical energy conversion technologies (fuel cells, electrolyzers for water splitting, carbon dioxide reduction reaction (CO_2RR), nitrogen reduction reaction (NRR), oxidation of various chemicals (COR), etc.) as effective and facile strategies have achieved remarkable progress [3, 4]. However, the efficiency of these devices is greatly limited by the sluggish kinetics, poor selectivity, low current density, or poor stability of the electrochemical reactions. Designing advanced electrocatalysts with high selectivity, activity,

Published online: 09 March 2024

and durability is key to promoting electrochemical energy applications [5]. Metal-based catalysts with different particle sizes, shapes, crystal structures, chemical composition, metal–support interactions, and metal–reactant/solvent interaction species show entirely different catalytic properties [6–8]. Particularly, metal catalysts with different sizes (single atoms, nanoclusters, and nanoparticles) significantly influence the catalytic behavior for various heterogeneous catalytic reactions [9, 10].

Nanoparticles (NPs) with a large size lower the utilization efficiency due to unavailable inner atoms. In practical industrial applications, the complicated multiple active sites on the surface of the nanoparticles located at edge sites, corner sites, and planes would result in an indistinct reaction pathway and a low catalytic selectivity [11]. Therefore, the size effect from NPs to single atoms has been extensively investigated to promote atom utilization efficiency and enhance electrocatalytic performance [12–14]. Single-atom catalysts (SACs) with unique catalytic activity and selectivity have drawn a broad interest in electrocatalysis due to their 100% atom utilization efficiency and tailorability of active sites at the atomic level [15, 16]. Compared with metal nanoparticles, single atoms supported on common carriers (carbon-based materials and metal oxides) can alter the adsorption energy of intermediates due to their oxidation character [17, 18]. For instance, Fe/N/C catalysts with single carbon-hosted FeN_4 moieties are highly active for the oxygen reduction reaction (ORR), which follows the inherently sluggish four-electron transfer process that originates from the free-energy linear relationships between the intermediates [19]. When the electrocatalyst's active site binds O* adsorbate more strongly, it also tends to bind similar OH* adsorbate more strongly. However, the discrete metal centers in SACs may not be favorable for catalytic reactions involving multiple reactant molecules or ensemble sites. For instance, some SACs cannot simultaneously promote efficient adsorption and activation of all intermediates in complex electrochemical processes (e.g., CO_2RR and NRR) [20]. This scaling relationship limit (SRL) is an unavoidable obstacle for pure SACs. Thus, the isolated atomic active sites could show low activity or inactivity for some catalytic reactions due to the lack of coordination with adjacent active sites. For example, different from the high performance of platinum (Pt)-based SACs for 2-electron formic acid oxidation reaction, Pt-based SACs have been reported to be electrochemically inert for the 6-electron methanol oxidation reaction [21]. For the thermal catalysis field, similar experimental results have also been reported. Li et al. found that uniform Ru_3 clusters stabilized by nitrogen species (Ru_3/CN) exhibit high catalytic activity and selectivity for the oxidation of 2-aminobenzyl alcohol to 2-aminobenzaldehyde, superior to that of the Ru single atom (Ru_1/CN) catalyst [22]. Therefore, SACs without metal–metal effects are not the best option for some heterogeneous catalytic reactions, and the corresponding atomic clusters could play a significant role in heterogeneous catalysis.

Nanoclusters and ultrasmall nanoparticles (NCCs), an emerging class of atomically precise nanomaterials, are considered a distinct group of intermediates between atoms and nanoparticles [23]. The nomenclature regarding the size boundaries between "nanocluster" and "nanoparticle" is currently not strictly defined. Broadly, a nanocluster is typically viewed as a tiny aggregate of atoms or molecules with a size below 2 nm. In this review, we mainly refer to "nanoclusters" and ultrasmall nanoparticles as metal species with sizes $\leq$ 2 nm and $\leq$ 5 nm, respectively. Unlike the metal atoms in large NPs with high metal–metal coordination numbers, NCCs with much higher atom utilization efficiency, are well known for their high density of low-coordinated metal active sites [24]. The novel geometric structures in NCCs play a vital role in enhancing the activity of electrochemical reactions, usually showing highly geometric/coordination structure dependence [25]. Compared with SACs, the multiple metal–metal interactions of NCCs result in uniquely distinct catalytic performances due to their abundant active sites for the adsorption and activation of various intermediates. The ensemble effect of atoms in the cluster promises to decrease the reaction barrier and improve catalytic selectivity [26]. It offers conditions and the possibility for breaking the scaling relations between adsorption energies of similar adsorbates through various strategies in nanocluster catalyst design, including the introduction of co-adsorbates, promoters, ligands, and new alloy structures [27, 28]. In addition, the NCCs with low nuclearity significantly reduce the complexity of revealing the real active sites and facilitate the exploration of new reaction pathways. To stabilize the nanoclusters and regulate their electronic structure, supported or ligand-coordinated NCCs have been intensely investigated as promising candidates in heterogeneous catalysis because of their exceptional catalytic capabilities [29–31]. The metal–support/ligand interactions can significantly induce interfacial charge transfer and electronic rearrangement due to the rich metal–support/ligand bonds, which further facilitate the optimization of the adsorption behaviors of intermediates [32]. The properties of metal nanoclusters vary nonlinearly depending on the specific interaction with carriers and the effects of electron confinement. However, in many cases, the specific atom-by-atom behavior is still not fully understood due to the challenge of spatially resolving the architecture and properties of low-nuclearity NCCs using existing analytical methods.

Extensive efforts have been devoted to investigating the catalytic properties of nanoclusters with rapid developments in theoretical modeling and advanced atomic-resolution characterization technology. With the rapid progress in this field, many new synthetic approaches have been reported

[33]. However, the controlled synthesis of nanoclusters with specific compositions and structures is considerably complicated. To date, literature reviews mainly focus on covering the NCC preparation methods. However, the surface chemistry engineering of NCCs in electrochemical applications has not been systematically summarized. Therefore, a detailed and up-to-date review in this field is necessary. Consequently, in this review manuscript, we attempt to elucidate the effects of atomic engineering and surface chemistry of NCCs for applications in some critical electrocatalytic reaction processes [34]. We hope that such a critical review can help accelerate research studies by presenting recent progress on the design and development of NCCs for electrochemical applications (e.g., ORR, oxygen evolution reaction (OER), CO_2RR, NRR and COR).

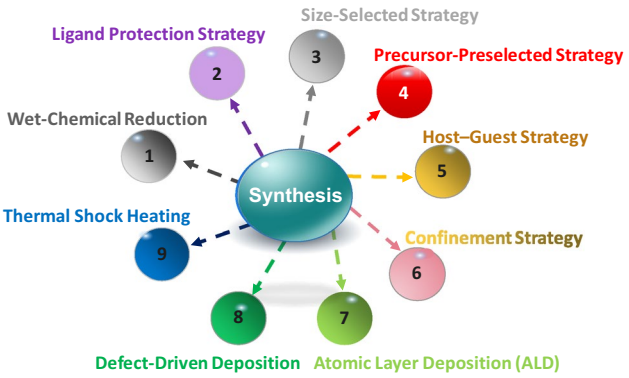

Fig. 1 Various nanoclusters and ultrasmall nanoparticles synthesis strategies

2 Synthesis of Nanocluster and Ultrasmall Nanoparticles

Since the term "nanochemistry" was first proposed in the 1990s, extensive research has been conducted on nanomaterials in the past several decades [35]. Various inorganic or inorganic–organic hybrid nanomaterials have been successfully synthesized and investigated. The knowledge about nanomaterials has made significant advances based on extensive research. To realize the controllable synthesis of metal clusters (e.g., the gold cluster, ruthenium cluster, palladium cluster, copper cluster, iron cluster and cobalt cluster), advanced synthesis strategies have been developed, such as the wet-chemical reduction, precursor-preselected strategy, host–guest strategy, confinement strategy, atomic layer deposition (ALD), ligand protection strategy, size-selected strategy, thermal shock heating method, and defect-driven deposition (Fig. 1) [36–40]. By carefully modulating the synthesis parameters to guarantee an appropriate and controllable nucleation process, precise control of the cluster size and composition of the metal nanocluster on the support is possible.

The synthesis of metal-based nanoclusters with specific morphology and coordination environment via wet-chemistry reduction is commonly realized by epitaxial growth. For instance, Sun et al. first synthesized Pd nanosheets and successfully grew Ir nanoclusters on the Pd nanosheets via a solution-phase epitaxial growth method [41]. Designing atomically monodispersed heterogeneous catalysts with uniform active sites remains a considerable challenge. The metal precursor selected for the wet-chemical reduction method significantly affects the structure of metal species. For example, using the (Ethylenediamine)iodoplatinum(II) dimer dinitrate and H_2PtCl_6 as the Pt precursors, Wang et al. successfully prepared a mesoporous graphitic carbon nitride (mpg-C_3N_4) supported dual-atom Pt_2 and single-atom Pt_1 catalysts, respectively [42]. In addition, molecules containing desirable metal atoms such as carbonyl bis(dicarbonyl cyclopentadienyl iron) ($Fe_2O_4C_{14}H_{10}$) [43], palladium chloride dimer ($[PdCl(C_3H_5)]_2$) [21], palladium acetate trimer ($[Pd(OAc)_2]_3$) [44], were also selected as the precursors. The wet-chemistry reduction as a facile approach enables the synthesis of metal nanoclusters on a large scale [29, 45, 46]. However, the precise control of the cluster size and composition is full of challenges. As a result, the broad size range of metal clusters breaks the metal clusters' structural uniformity, which reduces the metal atom utilization and decreases the mass-normalized catalytic activity. Some metallic cluster carbonyls have been widely used as precursors to prepare supported metal clusters by decarbonylation at elevated temperatures. For example, the metal–organic frameworks (MOFs) [47], dendrimers [39], and macromolecules[48] have well-defined structures that can spatially encapsulate metal complex through coordination bonding, porous confinement effect, and cations exchange. Significantly, the MOFs show many advantages and have been excellent platforms for preparing supported atomic clusters, such as nitrogen-coordinated dual-metal sites [49–54]. However, the dual-metal sites synthesized by pyrolyzing two metal precursors simultaneously face the challenge of precisely controlling each metal site's location. The N-doped carbon support combined with the atomic layer deposition (ALD) technique provides the possibility to achieve atomically ultrafine metal clusters, even bimetallic clusters [45, 55–58]. For example, Sun et al. employed the ALD technique to prepare Pt-Ru dimers on nitrogen-doped carbon nanotubes (NCNTs) (Fig. 2a) [40]. Through carefully controlling the deposition conditions, the second metal (e.g., Ru) can only attach to the first one (e.g., Pt), successfully forming the A–B bimetallic dimer structures (Pt–Ru dimers).

The surface engineering of metal nanoclusters by the ligand protection strategy has also been intensively studied and explored [30]. As the outermost layer, the surface

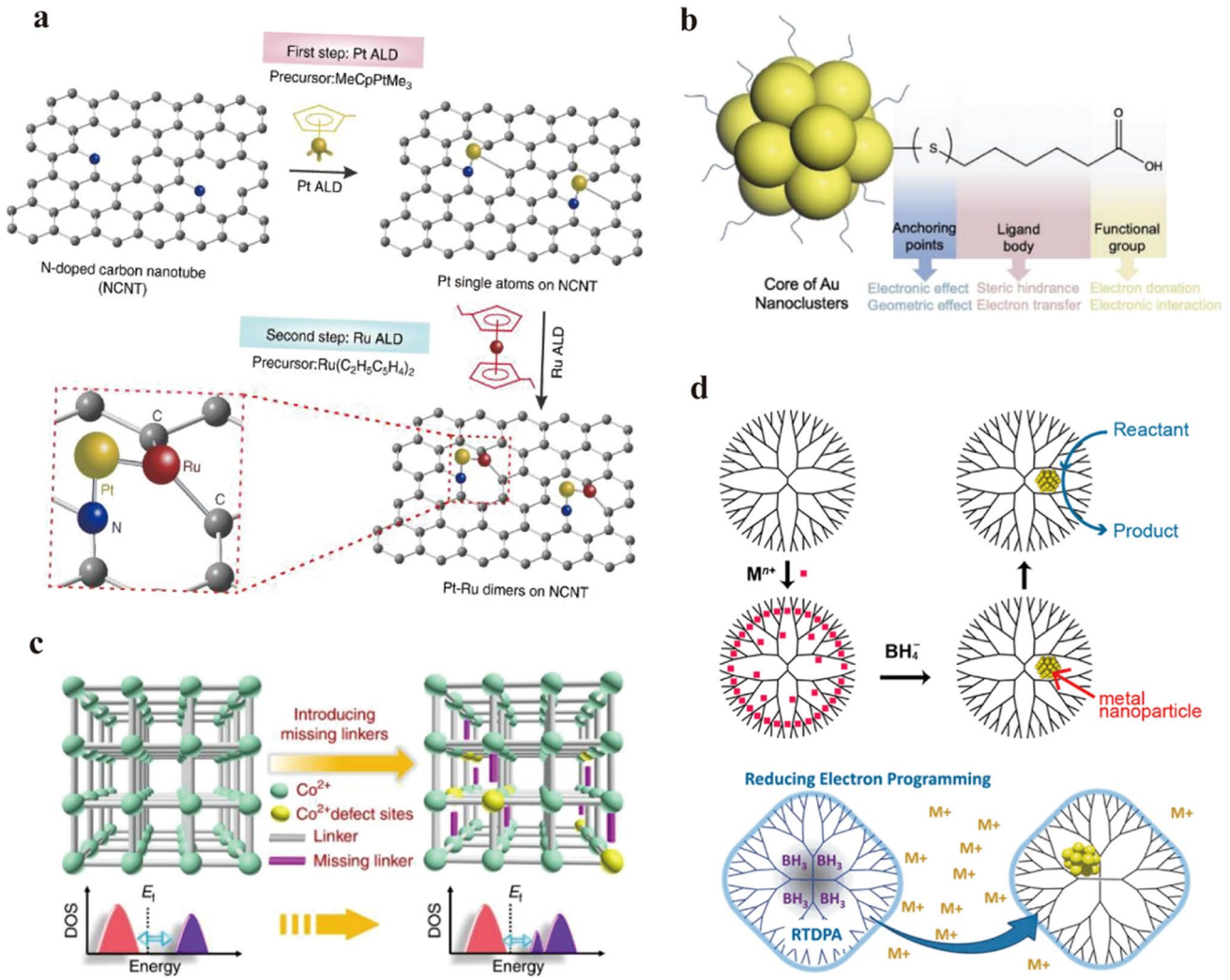

Fig. 2 **a** Schematic illustration of ALD synthesis of Pt–Ru dimers on nitrogen-doped carbon nanotubes. Reproduced with permission from Ref. [38]. Copyright 2019, Springer. **b** Schematic illustration of the three parts (anchoring point, ligand body, and functional group) of the protecting ligands on the cluster surface. Reproduced with permission from Ref. [37]. Copyright© 2021, Wiley–VCH. **c** Modulating electronic structures of MOFs via introducing missing linkers. Reproduced with permission from Ref. [38]. Copyright© 2019, Springer. **d** Conceptual image of reducing-capsule cluster synthesis and size control. Reproduced with permission from Ref. [39]. Copyright© 2020, American Chemical Society

ligands of metal NPs will directly interface with the external environment (e.g., electrolyte, reactant), determining their performance in various applications. The surface ligands can also block some active sites of metal clusters, which might have a negative effect on metal clusters' catalytic activity. However, a delicate design of the ligands on the clusters' surface has proved to be an effective way to enhance catalytic performance [37, 59, 60]. The unique "core–shell" structure with the metal core and ligand shell can also be used to design ligand-protected metal cluster catalysts with improved stability, selectivity, and activity [28]. Unlike bulk metal, which is highly stable in the external environment, single-metal clusters with ultrasmall size are very active in diverse chemical reactions, such as oxidation, hydrogenation, and coupling. The ligand layer on the metal surface plays a crucial role in improving the stability of metal clusters. The carefully selected ligands with specific anchoring points, ligand bodies, and functional groups effectively prevent metal clusters oxidative etching and aggregation in solution (Fig. 2b) [37]. The organic–inorganic hybrid materials (e.g., MOFs) with metal oxide cluster nodes or metal nitride cluster nodes can be directly used to catalyze some critical electrocatalytic reactions. The atomic clusters, via ligand protection from N or O coordination, generate defects by introducing missing linkers, significantly increasing their catalytic activity (Fig. 2c) [38]. The synthesis of metal nanoclusters with dendrimers is generally conducted by using the following steps: (1) metal ions

chemical adsorption on dendrimers, such as Cu^{2+}, Pt^{2+}, or Pd^{2+}; (2) $NaBH_4$ as a reducing agent to obtain dendrimer-encapsulated metal nanoclusters (Fig. 2d) [40]. On the contrary, the "reducing capsule" strategy is also employed. The dendrimer accumulates desired molar amounts of BH_3 as the reducing agent, which can provide a certain amount of electrons. By controlling the average number of metal ions or reducing agents accumulated in the dendrimer, a certain number of metal ions with the same electron transfer number are reduced to metal clusters. Compared with other chemical approaches, using dendrimers as templates to synthesize tiny clusters shows significant advantages in view of their synthetic precision and scalability.

Multimetallic nanoclusters (MMNCs; i.e., ultrafine nanoparticles with ≥ 3 elements) and ultrasmall nanoparticles have received great attention recently because of their multi-elemental composition [61–63]. However, conventional approaches to preparing MMNCs often lead to broader size distribution and inhomogeneous structures. The size and structural heterogeneity limit property optimization and mechanistic understanding. With increasing compositional complexity, the enormous challenge of controlling the kinetics of chemical reactions at the nanoscale results in inhomogeneous structures due to phase separation or elemental segregation. Based on the thermodynamic equation ($\Delta G = \Delta H - T \cdot \Delta S$), the formation of high-entropy nanoparticles involves competition between enthalpy and entropy gain (Fig. 3a) [63]. Namely, the high entropy gain in forming nanoparticles acts as a driving force for single-phase mixing. The enthalpy of the multi-elemental interactions (ΔH_{ij}) directly affects the resulting phase under near-equilibrium conditions (Fig. 3b). The wide range of possible composition and complex atomic arrangements create large challenges in controllable synthesis. Compared with conventional synthetic methods being typically time-consuming, random, and complicated, a robust and general synthesis of multimetallic nanoclusters is challenging but valuable to controllably tune the composition and systematically study MMNCs. Recently, a carbothermal shock technique with high-throughput (formulation in solution phases) and rapid synthesis (within seconds) has been reported to fabricate ultrafine multimetallic nanoclusters uniformly dispersed across the carbon support surface [64]. Through the flash heating and cooling of metal precursors on an oxygenated carbon support, Hu et al. reported a high-entropy-alloy (HEA) catalyst with uniform mixtures of multiple elements (Fig. 3c) [65]. The precursor-loaded carbon aerogel-carbon nanofiber film underwent shockwave heating through an electrical Joule heating process. This method allows for precise programming of temperature, on–off durations, and the number of repeated cycles. HEA nanoclusters synthesized by the carbothermal shock technique commonly have a narrow size distribution. This approach presents a new dimension for the development of multimetallic nanomaterials. HEA catalysts will be discussed in more detail in the following sections.

The defect-driven deposition using defects of the supports to anchor the metal nanoclusters has also been reported [67–69]. For instance, structural defects in carbon materials have recently been demonstrated to be an effective means to trap and stabilize reaction products [70]. The structural defects with high reducing capacity can spontaneously reduce the metal ions to clusters. Dai et al. demonstrated that carbon defects with a lower work function showed a higher reducing capacity than defect-free basal plane carbons [71]. Consequently, the triggered preferential adsorption and reduction of Pt ions at the carbon defect sites prevented the aggregation of Pt atomic clusters. However, the metal nanocluster catalysts tend strongly to grow into larger crystallites through the particle migration and coalescence (PMC) and/or Ostwald ripening (OR) processes, especially for high-temperature catalytic reactions [72]. The thermal sintering inevitably leads to the loss of active surface area and thus the catalyst deactivation. Recently, Liang et al. demonstrated that a sulfur-doped carbon matrix could effectively suppress the metal nanocluster sintering kinetics by retarding metal atom diffusion and nanocluster migration [66]. Figure 3d illustrates the approach to inhibit metal migration, coalescence, and ripening through the strong chemical interaction between the metal clusters and sulfur atoms doped in the sulfur–carbon (S–C) supports. In high-temperature reactions, metal nanoclusters on sulfur-free carbon support easily aggregate into larger particles. Interestingly, sulfur-doped carbon can stabilize ~ 1 nm metal nanoclusters (Pt, Ru, Rh, Os, and Ir) at temperatures up to 700 °C in a reductive atmosphere. The sulfur-containing carbon enhances the chemical/electronic interactions between the metal nanoclusters and the carbon support, which promotes outstanding sinter-resistant properties.

The synthesis of NCCs has made significant progress. However, some approaches heavily rely on sophisticated precision equipment, limiting their feasibility for large-scale production. Strategies such as being size-selected, being precursor-preselected, host–guest, and ALD are effective for precisely controlling the size and composition of metal nanoclusters. Among them, precursor-preselected, host–guest, wet chemical reduction, and thermal shock heating strategies are widely employed for industrial scalability. In addition, it is crutial to explore novel SCCs with unique atomic configurations. Undoubtedly, such exploration is key to advancing the investigation of catalytic systems under actual reaction conditions.

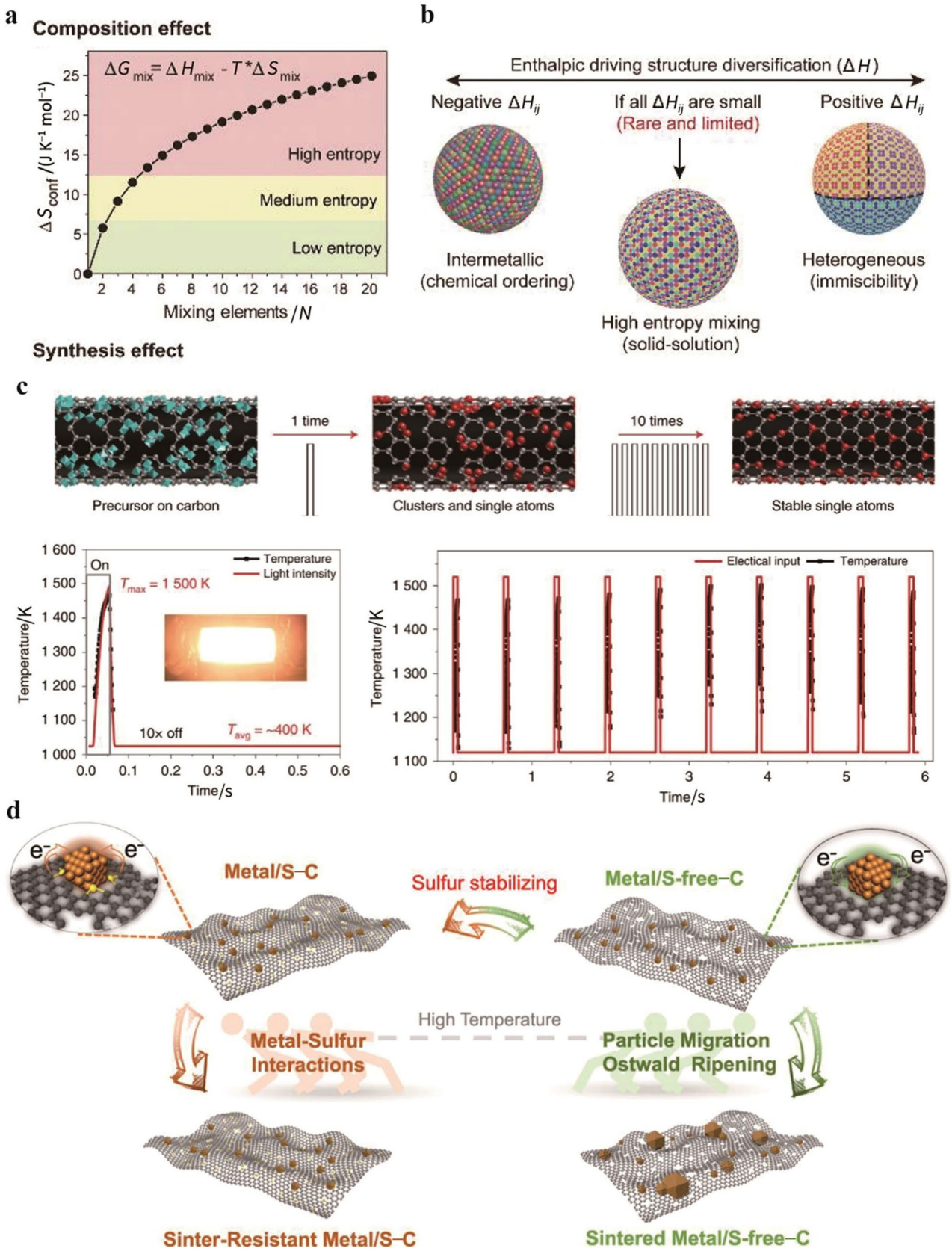
a
Composition effect
ΔG mix = Δ H mix - T*Δ S mix
ΔS conf /(J K⁻¹ mol⁻¹)
High entropy
Medium entropy
Low entropy
Mixing elements /N
b
Enthalpic driving structure diversification (Δ H)
Negative Δ H ij
If all Δ H ij are small
(Rare and limited)
Positive Δ H ij
Intermetallic
(chemical ordering)
High entropy mixing
(solid-solution)
Heterogeneous
(immiscibility)
Synthesis effect
c
1 time
10 times
Precursor on carbon
Clusters and single atoms
Stable single atoms
On
Temperature
Light intensity
T max = 1 500 K
10× off
T avg = ~400 K
Temperature/K
Time/s
Electical input
Temperature
d
Metal/S–C
Sulfur stabilizing
Metal/S-free–C
High Temperature
Metal-Sulfur
Interactions
Particle Migration
Ostwald Ripening
Sinter-Resistant Metal/S–C
Sintered Metal/S-free–C

◂**Fig. 3** **a**, **b** Thermodynamic analysis of HEAs considers both entropy **a** and enthalpy **b**. Reproduced with permission from Ref. [63]. Copyright© 2022, American Association for the Advancement of Science. **c** The schematic diagram of the thermal shock heating method. Reproduced with permission from Ref. [65]. Copyright© 2019, Springer. **d** Schematic illustration of the sulfur-stabilizing process. Reproduced with permission from Ref. [66]. Copyright© 2021, Springer

3 Effects of Surface and Interface Chemistry of NCCs on the Related Electrocatalysis Reactions

Developing high-performance NCCs depends on delicate architecture control and an in-depth understanding of the associated reactivity patterns. The novel geometric structures of NCCs can be built with metal–metal/oxygen/sulfur/nitrogen coordination [23, 73–79]. Surface geometric/coordination chemistry of nanoclusters has profound consequences on determining their catalytic properties [80]. Figure 4 illustrates the properties of atomic clusters supported on suitable carriers, such as the number of metal atoms, homo/heteronuclearity, protection by ligands, metal–support charge transfer, and local interactions, which all impact the electronic structure [54, 81]. The surface chemistry engineering of nanoclusters involves optimizing their geometric structure and electronic properties, which can be described from two perspectives (Fig. 5): (1) indirect modifications by interface bonding (support/ligand–cluster interactions); (2) direct modifications on nanoclusters (vacancy, heteroatom-doping, strain, size, multimetallic assembling, etc.) [54, 82, 83]. By identifying their general structural features, including the composition, nuclearity, coordination environment and location, and dynamic effects in reactive environments, researchers attempt to understand the correlation between the atomic structures of nanoclusters and their properties. The detailed investigation of geometric effects, electronic effects, and synergy effects can further promote atomic-precision engineering toward materials design. However, the irregular three-dimensional morphologies, complicated reaction conditions, non-uniform surface structures, and composition make it hard to build an accurate model of coordination sites. In many cases, researchers have to simplify the systems to reveal the effects of the engineering of nanoclusters. Moreover, the coordination chemistry of metal nanoclusters' surface with supports or ligands is essential in determining the catalytic performance of NCCs. Therefore, we also illustrate the critical roles of supports and ligands in improving the clusters' structural stability and catalytic activity: (1) optimizing their interfacial bonding; (2) promoting electron transfer; and (3) realizing support–cluster synergy effects.

3.1 Support/Ligand–NCCs Interactions (SLCIs) in Electrocatalysis Applications

Anchoring NCCs via chemical bonds on various supports or ligands is crucial to structurally stabilize NCCs, which also guarantees strong SLCIs [84–87]. The SLCIs would induce unique geometric, electronic, and synergy effects, which eventually change the catalytic performance [43, 88, 89]. The interfacial bonding between catalysts and supports/ligand plays a key role in minimizing particle aggregation and improving catalyst's stability. N-doped porous carbons, graphenes, carbon nanotubes, and MOFs have been widely used as supports [90]. The generated charge transfer between the metal and support can impact the adsorption energy of reaction intermediates and eventually improve the catalytic activity, selectivity, and stability.

M–N–C single-atom catalysts (where M = metal) have received great attention; thus, the Fe–N_4 active site is the most active component for ORR in acid. However, simultaneously improving the activity and stability of the Fe–N–C catalysts remains a significant challenge [19, 91–93]. Recently, the regulation of electron distribution of single-atomic metal sites by atomic clusters has shown great potential in improving the intrinsic activity and stability in the ORR [94–97]. For example, Shui et al. developed a Fe–N–C catalyst with nitrogen-coordinated iron clusters and Fe–N_4 active sites for ORR in an acid environment [94]. A model featuring a Fe_4–N_6 structure with a neighboring Fe-N_4 site has been illustrated in Fig. 6a. The $4e^-$ ORR pathway involves sequential intermediates O_2^*, OOH^*, O^*, and OH^*, as illustrated in Fig. 6b. After introducing iron clusters, theoretical calculations indicate that OH shows a strong affinity for adsorption onto Fe–N_4 active sites (Fig. 6c). Consequently, a permanent OH ligand grafted on Fe–N_4 increases the ORR intrinsic activity of the Fe–N_4 site by 60%. In addition, the suppression of the amplitude of Fe–N bonds by the strong electronic interaction between the cluster and the Fe single atom effectively reduces the demetalation of Fe–N_4 sites, resulting in an enhanced catalyst's long-term stability in PEMFCs (Fig. 6d). During a 150-h stability test conducted at 0.5 V, the catalyst exhibited a minor decrease. The SLCIs could also induce the spin-state transition of Fe single atoms, which is highly correlated with the demetalation durability and ORR activity of Fe–N–C electrocatalysts [96, 98–100]. For example, theoretical calculations indicate that introducing Pd nanoclusters induces the spin-state transition of single-atom sites from low spin to intermediate spin [96]. As a result, the facile removal of OH^* due to the strong electronic interaction suppresses the site-blocking effect and enhances the ORR activity. Theoretical research has proved that MnN_4 sites have improved stability relative to FeN_4 due to the weak Fenton reactions involving Mn ions in the acid condition [101, 102]. Recently, the combination

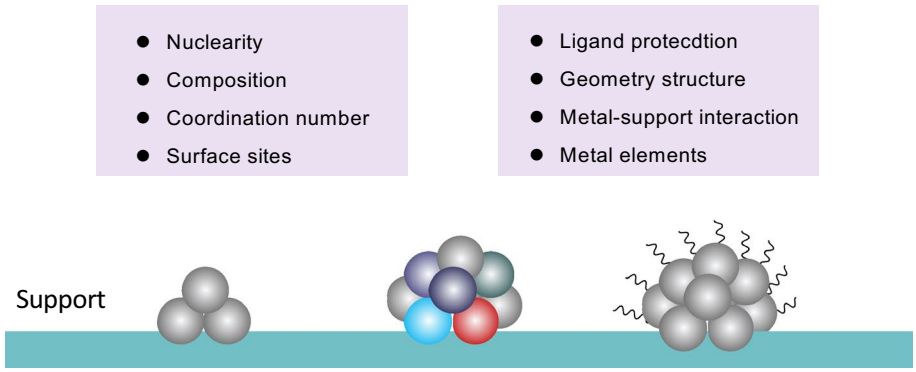

Fig. 4 Structural characteristics of supported low-nuclearity catalysts

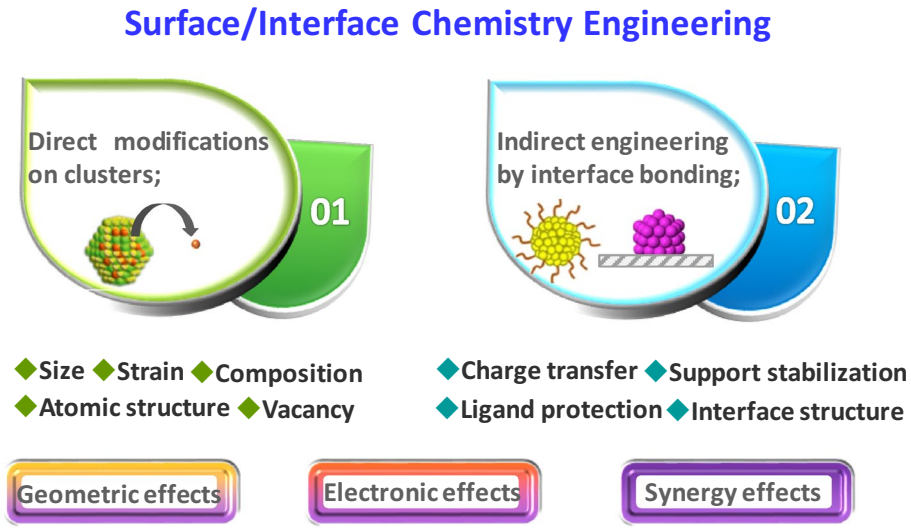

Fig. 5 The surface and interface chemistry engineering of nanoclusters by direct and indirect strategies

of atomically-dispersed Mn–N_4 sites and FeMn atomic clusters has been reported for efficient four-electron ORR [97]. The regulation of electron distribution of the Mn site by FeMn atomic clusters can facilitate the O–O bond-breaking process.

Similarly, the strong electronic interaction between clusters and single atoms has also been reported for the hydrogen evolution reaction (HER) [104, 105]. Liang et al. found the size-dependent charge transfer exists between the metal and the support [103]. By increasing the H_2-reduction temperature to 700 °C, uniform Pt nanoclusters with an average size of 1.56 nm homogeneously dispersed on the S–C support were obtained (PtNC/S–C) (Fig. 6e,f). Unlike the electron transfer from single platinum atoms to sulfur-doped carbons (about 0.069 electrons), the charge transfer reversal from carbon supports to Pt clusters occurred (0.657 electrons) (Fig. 6g, h). Moreover, by studying twelve hydrogen adsorption sites, they found that hydrogen adsorption sites on the electron-enriched state of Pt atoms exhibit an outstanding HER performance. Consequently, the electron-enriched Pt nanoclusters showed superior HER activity compared with electron-deficient Pt single atoms. The mass activity of PtNC/S–C (26.1 A mg^{-1}) was 27 times greater than that of PtSA/S–C (0.964 A mg^{-1}) (Fig. 6i). Besides this, Lu et al. developed Pt atomic clusters with Pt–O–Pt units anchored on Co–N–C support to form strong interactions for enhanced hydrogen evolution catalysis [105]. Theoretical calculations revealed that the significant electron transfer occurring at the Co–O–Pt interface resulted in a reduced electron density around these Co/Pt atoms, which is not beneficial for the HER activity. However, less charge delocalized from Pt to the nearby O atoms in Pt–O–Pt units rendered these Pt atoms having a higher electron density. Furthermore, after H^+ adsorption on the surrounding O linkers, the enhanced electron density around the nearby Pt further boosted the kinetics of HER on these Pt atoms. Furthermore, high H^* coverages on Pt–O–Pt units significantly decreased the free energies of H* (ΔG_{H^*}), which played an important role in the HER process.

The ligand–cluster interactions show great promise in designing advanced NCCs for many electrocatalytic reactions, such as HER, ORR, and CO_2RR [26, 107–110]. Metal nanoclusters protected by different types of ligands, such as thiolates [111–113], alkynyls [114–116], hydrides [117,

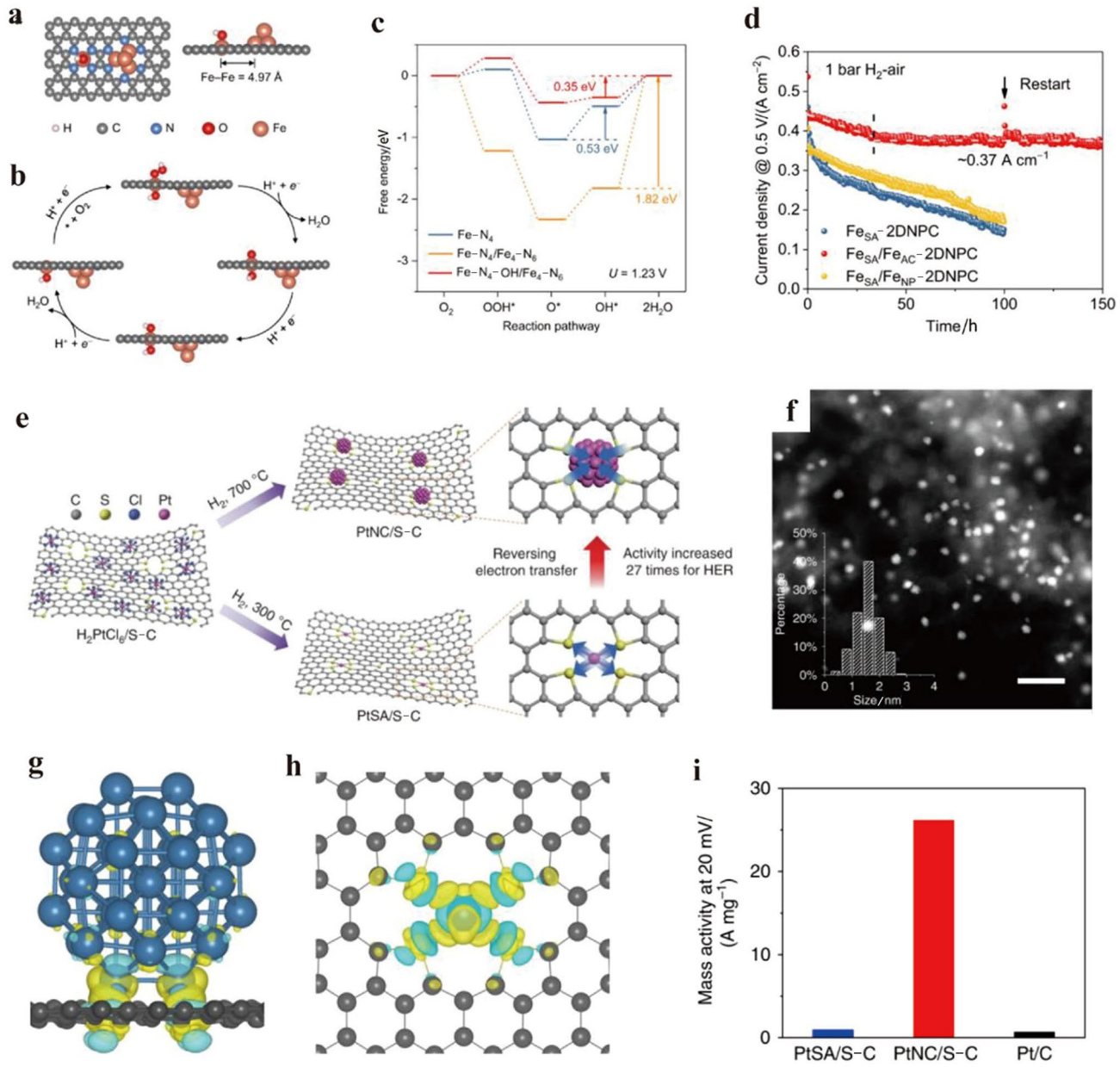

Fig. 6 **a** Model structure of Fe–N_4/Fe_4–N_6 used for theoretical calculation. **b** Schematic ORR process on the Fe–N_4 site of Fe–N_4–OH/Fe_4–N_6. **c** Free energy diagrams at 1.23 V for ORR. **d** The stability test in PEMFCs at a constant voltage of 0.5 V under 1 bar (1 bar = 100 000 Pa) H_2-air. Reproduced with permission from Ref. [94]. Copyright 2022, Springer. **e** Schematic model of the catalyst preparation process. **f** HAADF-STEM image of PtNC/S–C. (g,h) Difference charge density analysis of Pt_{38}/S-graphene and Pt_1/S-graphene system. **i** Mass activity at an overpotential of 20 mV. Reproduced with permission from Ref. [103]. Copyright© 2019, Springer

118], dithiophosphate [118], and *N*-heterocyclic carbenes [119, 120], have been reported to be the feasible preparation strategy. Interface structures induced by different ligands are important in affecting electrocatalytic activity, stability, and selectivity [106, 121]. For example, different from the S/Au interface of the Au-thiolate system with simple σ-coordination, the PhC≡C/Au interface of the Au-phenylacetylene (PhC≡CH) system features π-conjugation between C≡C and the substrate Au in addition to the σ-bonds [110, 122]. Compared with single nanocluster catalysts, metal nanoclusters synthesized by ligand engineering provide a well-defined core–shell structure, which may exhibit particular advantages for a specific reaction [28]. The unique structure achieved through independently engineering the core and shell is much more likely to exhibit suitable properties for electrocatalysis. These ligand shells of nanoclusters

should be quite open to allow small reactants to access the core surface readily. Through continuously well-identifying and understanding the ligand–cluster interfaces, the development of a new efficient electrocatalyst provides a powerful platform [24]. For example, to precisely fabricate bimetallic cluster catalysts with atomic-level control of dopants, Lu et al. report a strategy for the controllable synthesis of partially ligand-enveloped Au_4Pt_2 and Au_4Pd_2 clusters supported on defective graphene for exceptional electrochemical NRR [26]. Figure 7a shows the atomic structures of the $Au_4Pt_2(SR)_8$ clusters (R represents C_2H_4Ph), which can form a 1D polymeric chain-like structure. The removal of two ligands in $Au_4Pt_2(SR)_8$ creates two singly occupied electrons on the lower valent metal atoms, which may facilitate the electron transfer and N_2 activation (Fig. 7b, c). They evaluated the NRR performance of the as-prepared $Au_4Pt_2(SR)_8$ catalyst with graphene support, as illustrated in Fig. 7d. Compared to $Au_4Pt_2(SR)_8$, $Au_4Pt_2(SR)_6$/G shows a higher NRR activity with a high NH_3 yield at all the applied reduction potentials (Fig. 7e). Specially, the $Au_4Pt_2(SR)_8$ catalyst achieved a maximum NH_3 yield of 7.9 μg mg^{-1} h^{-1}, as shown in Fig. 7e.

Surface ligand shells on nanostructured Cu catalysts are also crucial to enhance CO_2RR selectivity at low overpotentials. For instance, Jiang et al. investigated the lattice-hydride mechanism of CO_2 reduction on

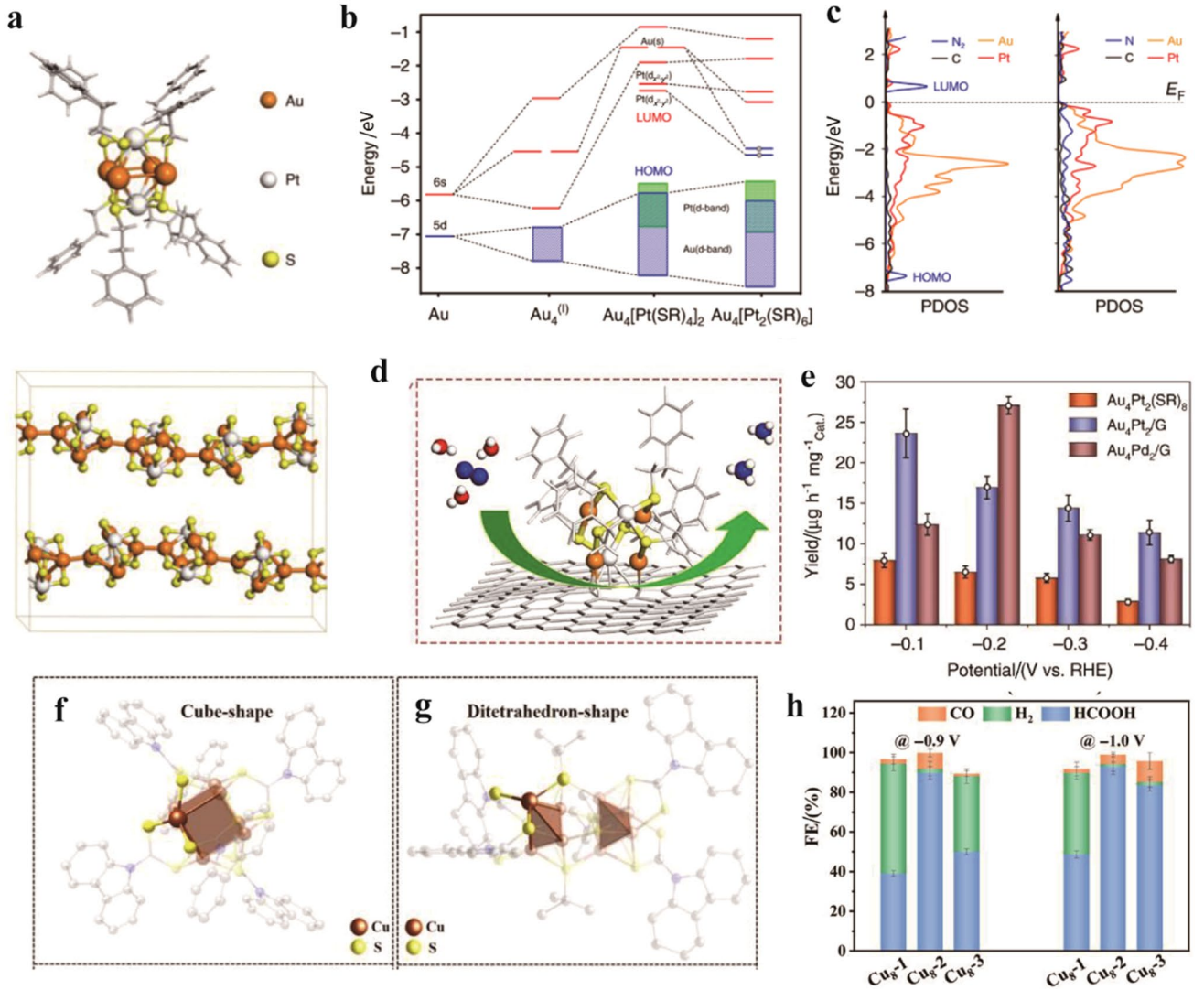

Fig. 7 **a** Atomic structures of the clusters. **b** Schematic energy-level diagram of unsupported $Au_4Pt_2(SR)_8$ and $Au_4Pt_2(SR)_6$ clusters. **c** Calculated PDOS of Au_4Pt_2/G catalysts without and with N_2 adsorption. **d** Schematic illustration of the Au_4Pt_2/G catalysts for NRR. **e** NH_3 production rate. Reproduced with permission from Ref. [26]. Copyright© 2020, Springer. **f**, **g** Perspective views of the Cu_8 NC structures for the cube-shaped Cu_8-1 and ditetrahedron-shaped Cu_8-2 NCs. **h** FEs for HCOOH, CO, and H_2 at potentials of − 0.9 and − 1.0 V. Reproduced with permission from Ref. [106]. Copyright© 2022, Wiley–VCH

ligand-protected Cu-hydride nanoclusters ($Cu_{32}H_{20}L_{12}$, L: the dithiophosphate ligand). Theoretical analysis indicated that the presence of negatively charged hydrides in the copper cluster plays a critical role in determining the high selectivity towards the production of HCOOH instead of CO at low overpotentials. Zang et al. successfully synthesized structurally precise Cu_8 cluster isomers with cube- and ditetrahedron-shaped core structures, respectively (Fig. 7f, g) [106]. The ditetrahedron-shaped Cu_8 clusters exhibited a higher selectivity and Faradaic efficiency than the cube-shaped Cu_8 cluster, achieving Faradaic efficiencies (FE_{HCOOH}) of 90% at − 0.9 V and 92% at − 1.0 V, as indicated in Fig. 7i. Suppressing the competing HER is crucial to enhance CO_2RR selectivity. Theoretical investigations demonstrate that the low fraction of H_2 in the reduction products on the ditetrahedron-shaped Cu_8-2 is due to the higher energy barrier for the H_2-formation. In addition, the unique structure of the ditetrahedron-shaped Cu_8 cluster is more feasible for catalytic HCOOH production rather than CO, due to the moderate energy barrier.

Anchoring SCCs onto various supports or ligands through chemical bonds is crucial for their structural stabilization. This stabilization is essential for ensuring robust interactions between the support and the clusters, significantly enhancing the performance of various electrochemical reactions. The interactions between the support and the clusters lead to distinct geometric, electronic, and synergistic effects, which are crucial in determining the superior catalytic performance of NCCs. However, regulating the interfacial bonding of support/ligand–NCC remains challenging and requires further systematic exploration.

3.2 Atomical Engineering of Nanoclusters or Ultrasmall Nanoparticles (AENs) in Electrocatalysis Applications

Nanocluster and ultrasmall nanoparticle catalysts (NCCs) characterized by definite low-nuclearity metal active centers currently emerge as rising stars [20, 22, 105]. NCCs with an ensemble of metal atoms provide diverse combinations of multiple metal atoms, constructing rich surface sites for the adsorption of specific reactants/intermediates. Compared with NPs with continuous metal valence bands, atomic clusters with two or more atoms show unique geometric and electronic structures. The discrete electronic states lead to higher Fermi energy levels (εF) and lower work functions, facilitating electron transfer from the clusters to adsorbates [123]. Therefore, the critical step of activation of reactants becomes easier. In addition, for the supported NCCs, metal atoms are exposed as much as possible and are available for the reactant molecules due to their extremely low nuclearity [124]. Based on the different properties of metal nanoclusters or ultrasmall nanoparticles, such as the atomic number, morphology, size, composition, surface defects, and structure, we will gain insight into different kinds of NCCs (Fig. 8).

3.2.1 Sub-Nanometer Clusters (SNCs)

Numerous studies have shown that nanomaterials' geometries and physicochemical properties highly depend on their size [125]. Therefore, a deep understanding of the related size-dependent properties is necessary to design efficient nanomaterials. When the size of conventional nanomaterial is reduced to the molecule level, some unprecedented and novel features have been observed. Vajda et al. found that the

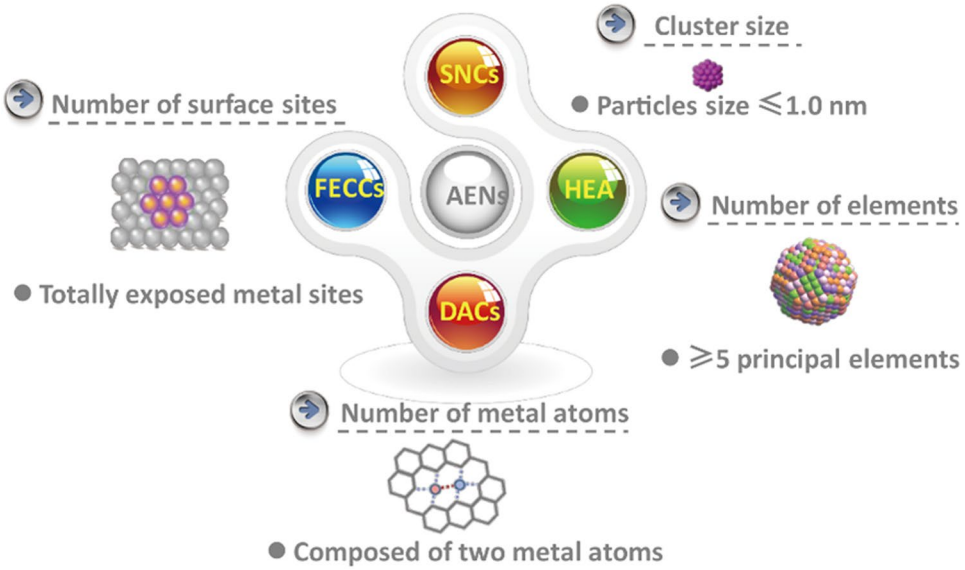

Fig. 8 Different kinds of NCCs based on the different properties of metal nanoclusters

overpotential and turnover frequency of sub-nanometer Pd clusters (Pd_4, Pd_6, and Pd_{17}) for OER in alkaline conditions are strongly size-dependent [126]. Based on the grazing incidence X-ray absorption spectroscopy results, the real active species of the supported Pd_4 and Pd_6 clusters during OER are stable Pd_4O_4 and Pd_6O_6 clusters. Theoretical calculations suggest that the OER reaction occurs on the bridging Pd–Pd sites for Pd_6O_6. To specify the unique size-dependent properties in depth, sub-nanometer materials as a bridge between conventional nanomaterials and molecules have increasingly been widely investigated [127–130]. There is currently no critical restriction on the size level for the sub-nanometer materials. It is widely accepted that the particle size smaller than 1.0 nm can be defined as sub-nanometer clusters [131]. Conventional characterization tools are challenging to determine the size accurately, especially at this extremely small scale. Prof. Wang considers that the so-called sub-nanometer materials (SNMs) should meet two aspects: (1) the size of SNMs confined should be at the atomic or molecular level; (2) SNMs should show unique size-related properties [132]. SNMs commonly include 0D sub-nanometer clusters (SNCs), 1D sub-nanometer wires (SNNs), and 2D sub-nanometer sheets (SNSs) [133]. SNCs with limited nuclearity can be seen as a kind of special molecule containing a multimetallic core. Moreover, due to the limited atomic number, the defects, heteroatom-doping, and metal–support/ligand interaction play significant roles in determining the properties of the whole sub-nanometer clusters [126, 134].

In the electrochemical reduction of the N_2 to NH_3, SNCs as efficient catalysts have also drawn attention [127, 136, 137]. Theoretically, the N_2 activation process is commonly considered the rate-determining step (RDS) due to the high-energy triple-bond in N_2, high ionization potential, and poor electron affinity of N_2. SNCs featuring multiple metal–metal interactions can lower the energy barrier of N_2 activation and increase the rate of the RDS. Using nanoreactors with internal cavities to encapsulate multiple active species has shown significant advantages [138, 139]. Recently, graphitic carbon nitride (C_3N_4) with regular surface cavities to encapsulate metal clusters has been reported [139–141]. For example, precisely confining sub-nanometer FeCu clusters in the extremely narrow cavities of C_3N_4 has been realized [127]. The homogeneously distributed bright spots indicate the presence of atomically dispersed metal sites (Fig. 9c). As depicted in Fig. 9a, when a N_2 molecule is adsorbed onto these sub-nano reactors containing triple metal atoms, it is stabilized by the interaction with all three metal atoms simultaneously, rather than just a single metal atom (Fig. 9a). The unique Fe-Cu coordination of the FeCu cluster effectively modifies the N_2 adsorption, turning the RDS from the hydrogenation ($NH^* \rightarrow NH_2^*$) and N_2 adsorption to the initial hydrogenation ($N_2^* \rightarrow N_2H^*$), characterized by a lower energy barrier (Fig. 9b). The significantly enhanced NRR performance with a nearly doubled production rate and 34% Faradic efficiency at 0.8 V versus Ag/AgCl is achieved (Fig. 9d, e). In addition, Qian et al. have also demonstrated the key role of introducing cobalt single clusters in altering the rate-determining step of ammonia synthesis from N_2 cleavage to proton addition (Fig. 9f) [135]. The cobalt clusters dispersed in nitrogen-doped carbon (CoSC–N–C) were successfully fabricated, which is revealed by the dark-field TEM image (Fig. 9g). Only small energy barriers in the whole nitrogen fixation process greatly facilitate the electron transfer and lead to a desirable NRR performance, reflected by a high ammonia production rate (76.2 μg h^{-1} $mg^{-1}_{cat.}$) and a high Faradaic efficiency (52.9%) (Fig. 9h, i).

When the size of clusters reduces to a sub-nanometer scale, they tend to aggregate into large particles. Appropriate substrates have proven to be key to stabilizing sub-nanometer clusters and preventing self-aggregation [142]. Mai et al. reported a 3D crumpled paper-like MXene, which not only effectively minimizes the self-stacking of 2D MXene nanosheets but also guarantees the total exposure of sub-nanometer Pt clusters (Fig. 10a, b) [143]. The induced strong electron transfer from Pt to MXene weakens the hydrogen adsorption. Consequently, the low platinum loading achieves much higher HER performance, about seven times that of commercial Pt/C (Fig. 10c). Lou et al. also constructed a stable electrocatalyst for HER by confining sub-nanometer Pt clusters in hollow mesoporous carbon spheres (HMCSs) [128]. They fist synthesized $Pt_5(GS)_{10}$ clusters, where GS represents deprotonated glutathione. These clusters were incorporated into the pore channels of hollow mesoporous carbon spheres (HMCSs), as depicted in Fig. 10f. The majority of the Pt clusters remain in the sub-nanometer range, approximately 0.77 nm in size (Fig. 10d, e). The mesoporous channels of carbon support effectively stabilize the highly active Pt clusters during ligand removal and maximize the utilization of the precious Pt atoms. X-ray photoelectron spectroscopy (XPS) revealed the coexistence of Pt^0 and Pt^{2+} in Pt clusters. The distinct electronic structure of Pt sub-nanometer clusters with enhanced mass transport leads to a remarkable HER performance in both acidic and alkaline solutions.

The ensemble effect, arising from interactions among two or more types of atoms within a single cluster, is highly desirable for complex multielectron reactions. However, manipulating and analyzing the structures of these sub-nanometer clusters remains a significant challenge. This difficulty primarily stems from the complexities involved in stabilizing precise quantities of diverse atoms within a single cluster.

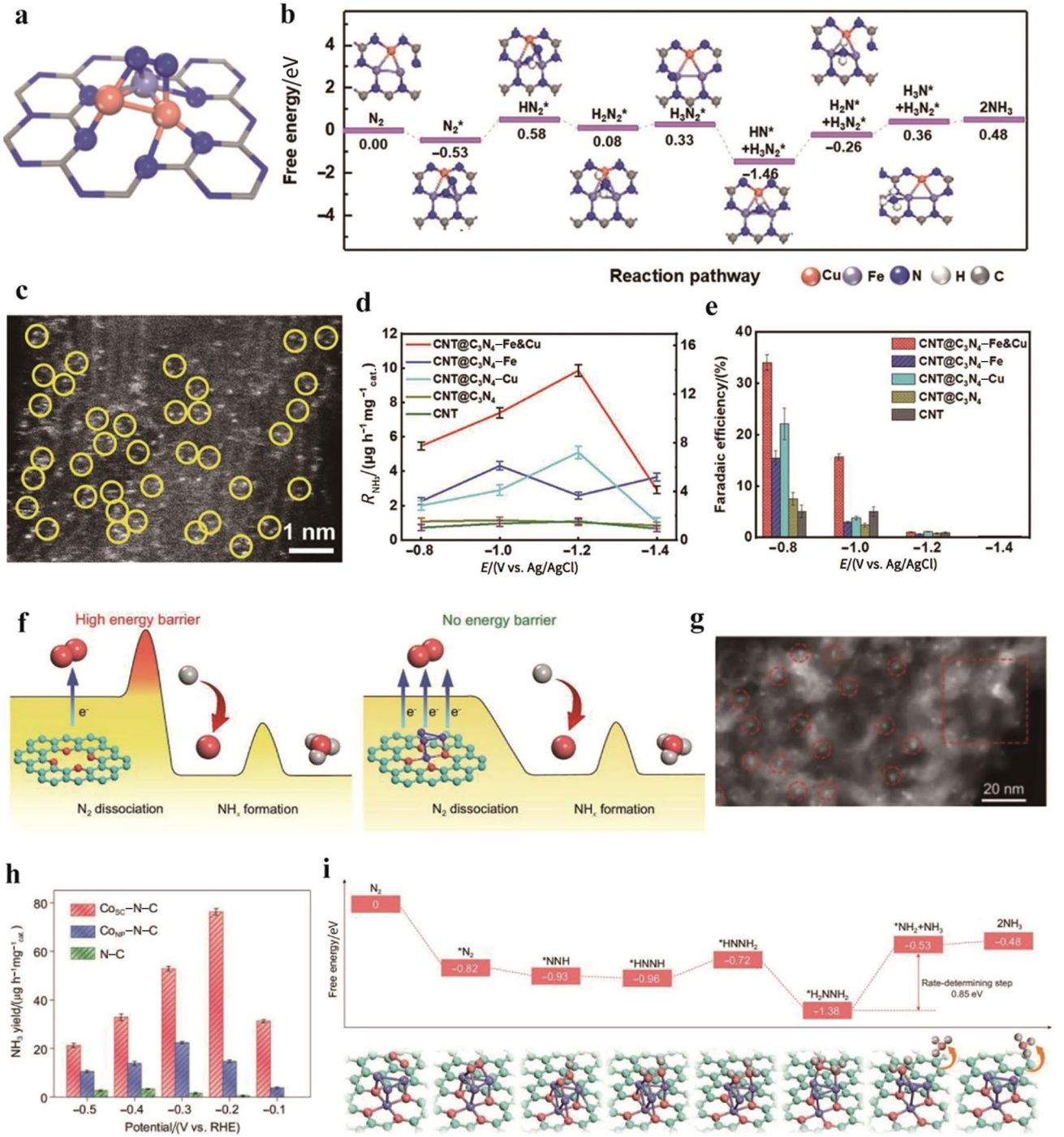

Fig. 9 **a** Adsorption configuration of a N_2 molecule over an atomic reactor with three metal atoms. **b** Free energy diagrams of NRR on Fe_2Cu clusters. **c** TEM image of CNT@C_3N_4–Fe&Cu. **d** NH_3 yield rates and partial current densities of the materials at different potentials. **e** Faradaic efficiencies of the materials at different potentials. Reproduced with permission from Ref. [127]. Copyright© 2021, American Chemical Society. **f** Schematic illustration for the mechanism of enhanced NRR activity by introducing Co single clusters in nitrogen-doped carbon. **g** Dark-field TEM image of Co_{SC}–N–C showing highly dispersed Co single clusters. **h** NH_3 yield rates at each given potential of Co_{SC}–N–C, Co_{NP}–N–C, and N–C. **i** Free energy diagram and models on Co_4–N_4/C. Reproduced with permission from Ref. [135]. Copyright© 2020, Oxford University Press

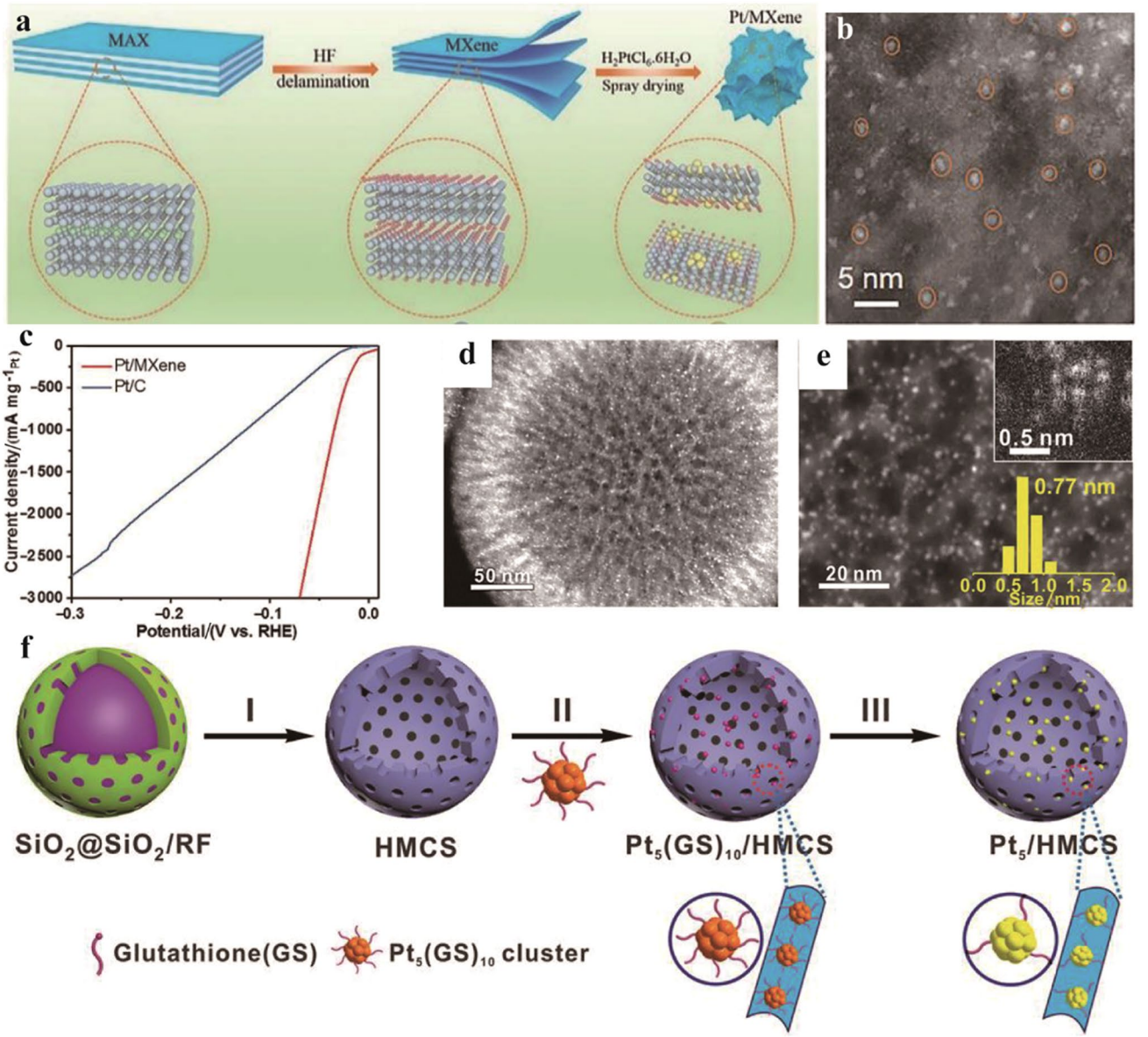

Fig. 10 **a** The preparation process of Pt/MXene. **b** HAADF-STEM images of Pt/MXene. **c** The mass activity of Pt/MXene and Pt/C. Reproduced with permission from Ref. [143]. Copyright 2022, Wiley–VCH. **d** ,**e** HAADF-STEM images Pt_5/HMCS. **f** Schematic illustration of the synthetic procedure of Pt_5/HMCS. Reproduced with permission from Ref. [128]. Copyright 2019, Wiley–VCH

3.2.2 High-Entropy Alloy (HEA) Catalysts

MMNCs offering unique and tailorable surface chemistries hold great potential for many catalytic applications [144–146]. Most metal-based nanoparticles studied comprise three or fewer metal elements to avoid synthetic complexity and structural heterogeneity. Recently, HEA materials (typically five or more principal elements in a single-phase solid solution) offering complex atomic configurations have emerged as novel catalytic materials due to their high activity and stability [147]. Figure 11a shows that pure metal (e.g., Co, Mo, Fe, Ni, and Cu) exhibits sharp peaks in the binding energy distribution patterns. In comparison, due to the electronic hybridization, HEA catalysts with multiple element mixing (e.g., CoMoFeNiCu) feature broad peaks and a nearly continuous spectrum for their adsorption energy. HEA catalysts with widely tunable electronic structures, diverse adsorption sites, and tunable binding energies show unique properties toward high-performance catalysis [148–150]. Their flexible composition range and homogeneously mixed solid-solution state provide a unique microstructure for property optimization via synergistic interactions among different elements, which could provide opportunities to

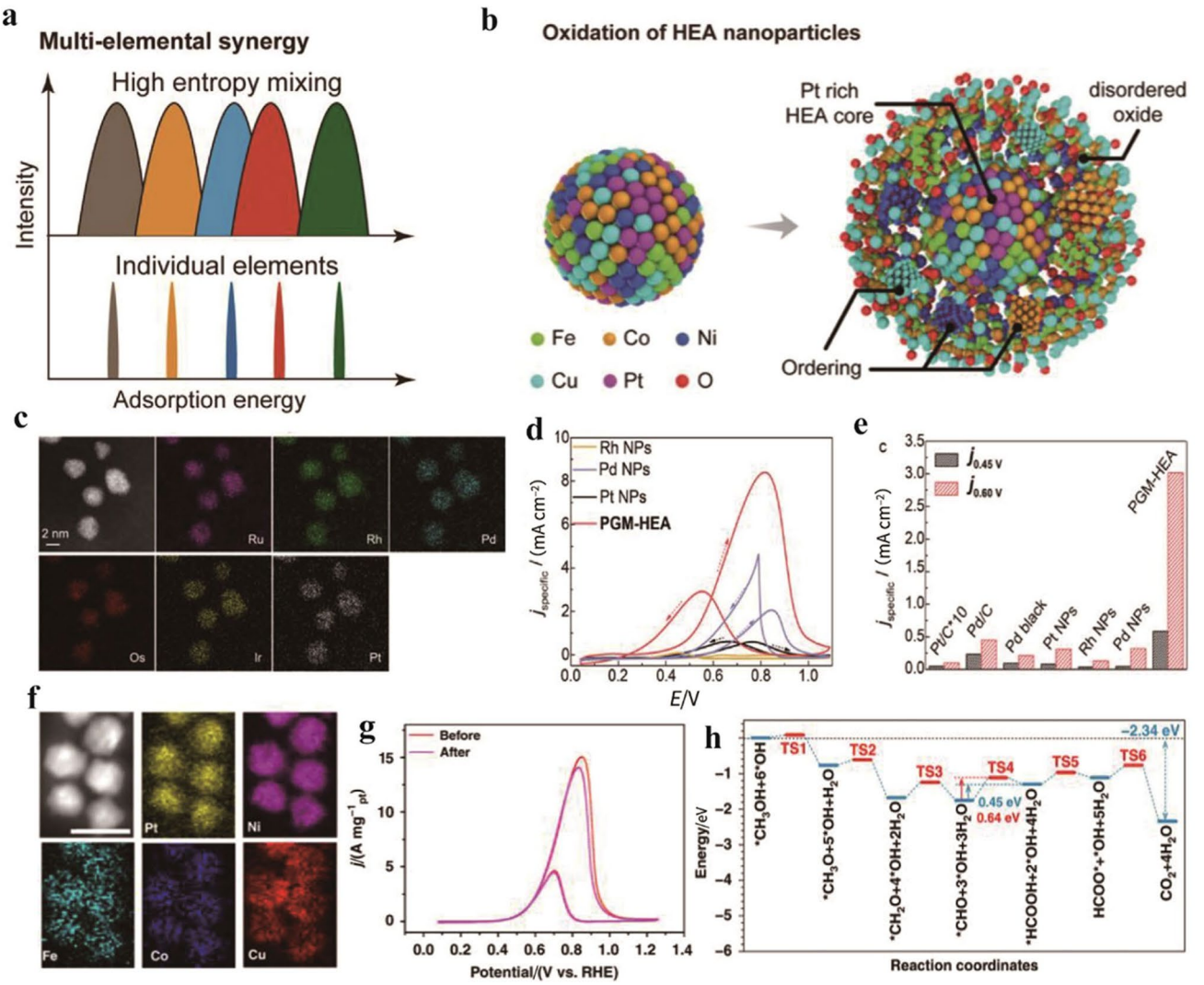

Fig. 11 **a** Multielemental synergy in high-entropy nanoparticles leads to a broadband binding energy distribution pattern. Reproduced with permission from Ref. [63]. Copyright© 2022, American Association for the Advancement of Science. **b** Schematic illustration of the oxidation process of HEA NPs. Reproduced with permission from Ref. [161]. Copyright© 2020, American Chemical Society. **c** HAADF-STEM images of the PtPdRuRhOsIr. **d** ,**e** Comparison of the ethanol oxidation reaction (EOR). Reproduced with permission from Ref. [151]. Copyright© 2020, American Chemical Society. **f** Elemental mappings of $Pt_{18}Ni_{26}Fe_{15}Co_{14}Cu_{27}$ nanoparticles. **g** Methanol oxidation reaction (MOR) performance of the $Pt_{18}Ni_{26}Fe_{15}Co_{14}Cu_{27}$/C. **h** Energetic pathway of the alkaline MOR. Reproduced with permission from Ref. [155]. Copyright© 2020, Springer

circumvent the SRL [63]. For example, Wu et al. found that the prepared IrPdPtRhRu HEA catalyst displayed high HER performance, and its turnover frequency was far beyond what was expected by traditional SRL theories [151]. Kitagawa et al. also fabricated a homogeneous IrPdPtRhRu HEA nanocluster using a continuous-flow reactor, which provides a new methodology for the fabrication of ultrasmall HEA [152]. A 1 nm-sized HEA nanocluster showed a remarkably high HER activity with a very small overpotential [148]. In addition, HEA with multifunctional active sites for the adsorption of multiple reaction intermediates is a particularly promising catalyst for tandem and complex reactions, such as the CO_2RR, ORR, NRR, and the oxidation of various chemicals [148, 153–156]. Wang et al. revealed the importance of multifunctional active sites for overall efficient NH_3 synthesis based on the $Ru_{22}Fe_{20}Co_{18}Ni_{21}Cu_{19}$ HEA [157]. Fe sites are in charge of N_2 adsorption and dissociation, whereas the nearby Co–Cu and Ru–Ni pairs are suitable for H_2 adsorption and dissociation, which contribute to high activity and selectivity in the NRR ($N_2 + 3H_2 \rightarrow 2NH_3$). In addition, in the ethanol oxidation reaction involving a complex 12-electron transfer and diverse intermediates, PtPdRuRhOsIr (PGM-HEA) demonstrated a much higher activity and

selectivity to complete oxidation to CO_2 than monometallic catalysts [151, 158, 159]. The HAADF-STEM image and EDX reveal that a single-phase solid-solution alloy is formed with a narrow size range (3.1 ± 0.6) nm (Fig. 11c). Among the catalysts tested, thePGM-HEA exhibited the highest specific current density across all potential ranges (Fig. 11d). Notably, at 0.6 V, the current density of PGM-HEA is 1.5 times higher than that of the highly active Au@PtIr/C catalyst (Fig. 11e). High-entropy mixing can improve structural stability at high and low temperatures. Specifically, a more pronounced $T\Delta S$ term ($\Delta G = \Delta H - T\Delta S$) at high temperatures benefits the formation and stabilization of high-entropy nanoparticles. Furthermore, the mismatch of the different elements and resultant lattice distortion would cause large diffusion barriers, tending to effectively prevent phase segregation at low temperature [160]. However, surface oxidation or reconstruction can occur in harsh conditions on the surface of HEA, resulting in a stable HEA-core and oxide-shell structure (Fig. 11b) [63, 161]. Nevertheless, HEA features improved structural stability compared with their fewer-element counterparts, potentially providing enhanced stability for both reduction and oxidation reactions. For example, Lai et al. developed uniform HEAs $Pt_{18}Ni_{26}Fe_{15}Co_{14}Cu_{27}$ (~ 3.4 nm) by a simple low-temperature oil phase strategy [155]. The lower heat of formation and similar atomic radii of Ni, Fe, Co, and Cu are in favor of stable HEA formation. Figure 11f demonstrates a uniform distribution of Pt, Ni, Fe, Co, and Cu elements within the HEA nanostructure. The HEAs catalyst showed high bi-functional electrocatalytic activity and stability for HER and methanol oxidation reaction (MOR) in the alkaline medium. After 1000 CV cycles, the mass activity of the $Pt_{18}Ni_{26}Fe_{15}Co_{14}Cu_{27}$/C catalyst for MOR decreased by only 6.4% (Fig. 11g). Theoretical calculations reveal different contributions from each element in HEA for the electrocatalysis process, which indicate the importance of the multi-active sites on the HEA surface. In the MOR process, the rate-determining step is the transition from [$CHO^* + 3OH + 3H_2O$] to [$HCOOH + 2OH + 4H_2O$], and the MOR process is exothermic (Fig. 11h).

Overall, their tunable composition, electronic structure, and impressive stability in corrosive environments render them promising candidates for advanced electrocatalysts. Although there is a rapidly growing interest in ultra-small HEAs, their exploration in electrocatalysis is a relatively recent development. Notably, the synthesis methods for ultra-small HEAs are complex and lack general applicability. Moreover, detailed structural information of HEA catalysts remains largely unexplored, and their complete catalytic potential is yet to be sufficiently investigated. The complex catalytic mechanisms underlying HEAs also require clearer elucidation. Therefore, an urgent need exists for a more rational design of HEAs to establish them as truly advanced catalysts. This will accelerate research and development in the field of electrocatalysis, leveraging the unique properties of HEAs.

3.2.3 Heteroatom Coordinated Dual-Atom Cluster Catalysts

Dual-atom catalysts (DACs) with the lowest nuclearity of metallic atoms have gained much attention, since they can exhibit better catalytic performance than simple SACs while maintaining the advantages of SACs, like 100% catalyst utilization efficiency [162–164]. DACs on carbon support have been reported to be efficient catalysts for CO_2RR, ORR, OER, and HER. Compared with SACs tending to agglomerate due to their increased surface free energy, the strong chemical interactions between the two neighboring atoms in the DAC can effectively prevent the atoms' agglomeration, enabling more versatile bonding interaction of molecules with the catalyst [33]. Moreover, the highly stable dual metal active sites on the support provide moderate adsorption of reactant molecules, enabling higher catalytic activity and selectivity [165]. Depending on the dual-metal composition, dual-metal sites in DACs can be divided into two homometal sites and two heterometal sites (Fig. 12b) [166]. Depending on the structure of dual-metal sites, they can be divided into two linked metal sites and two separated ones [166, 167]. Designing DACs by thermal polymerization and the precursor-preselected strategy has been widely reported [168–170]. However, the undesired thermal atomic migration during the synthesis process will result in poor uniformity of dual metal sites, significantly limiting their further application.

Recently, Leng et al. reported an interfacial cladding strategy to successfully construct well-defined Fe_2, Cu_2, and Ir_2 sites for ORR [169]. The interfacial cladding of polydopamine on ZIF-8 with metal dimer molecules effectively prevents the thermal migration of metal atoms during pyrolysis. The uniform nitrogen coordinated dual-atom Fe sites formed at 900 °C exhibit remarkable activity for electrocatalytic ORR in both alkaline and acidic media. The improved ORR performance stems from dual-atom Fe sites' excellent O–O activation ability. DACs have also attracted much attention in electrocatalytic CO_2RR, showing a great advantage over SACs [168, 171–176]. For instance, Ni, Co, Fe, and Cu SACs on nitrogen-doped carbon have been widely investigated for CO_2RR [177–179]. Fe SACs exhibit a low onset potential but suffer from low Faradaic efficiency and poor stability due to the strong binding of the Fe site and reaction intermediates (e.g., CO). Dual Fe atom sites allow reaction intermediates to simultaneously adsorb on dual-metal sites, which provides favorable conditions for breaking the SRL based on conventional SACs [166, 173]. Ni SACs show a high intrinsic catalytic activity and Faradaic efficiency (FE) for CO production [180, 181].

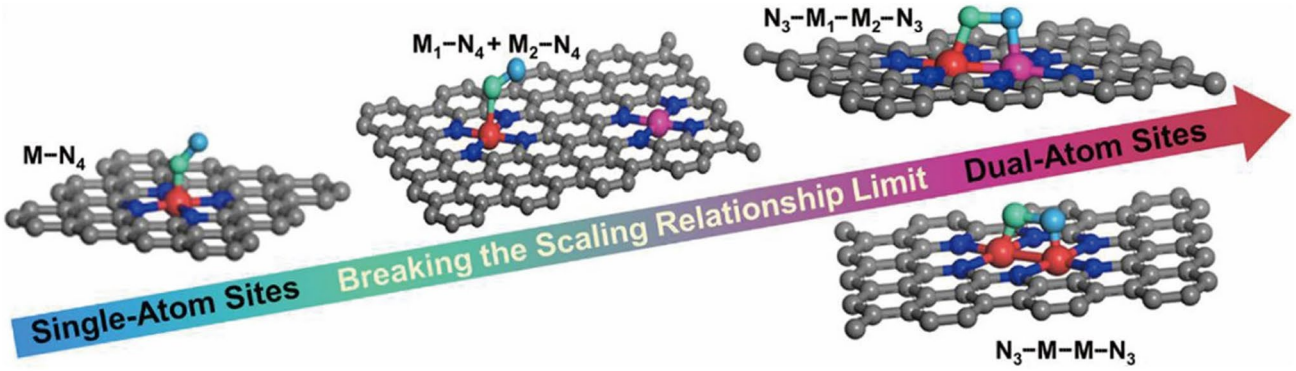

Fig. 12 Adsorption forms of intermediates in SACs and DACs. Reproduced with permission from Ref. [166]. Copyright© 2022, American Chemical Society

However, the large onset potential due to the high energy barrier to form the *COOH intermediate limits their practical application. Ni dual-atom catalysts can achieve efficient electrocatalytic CO_2 reduction with a high CO partial current density and high turnover frequency [176, 182]. In situ X-ray absorption and theoretical calculations have confirmed the existence of electron-rich active centers, indicating that the triggered adsorption of hydroxyl (OH_{ad}) of Ni dual-atom sites guarantees a moderate reaction kinetic barrier for the *COOH formation and *CO desorption [176]. In addition, by using operando synchrotron X-ray absorption spectroscopy, Yao et al. identify the dynamic catalytic center with oxygen-bridge adsorption on the Ni_2–N_6 site (O–Ni_2–N_6) for CO_2RR. Using operando synchrotron radiation Fourier-transform infrared (SR-FTIR) spectroscopy and DFT calculations, they propose a reaction pathway for the CO_2RR at the O–Ni_2–N_6 active site. As shown in Fig. 13a. The Ni_2–N_6 structure adsorbs oxygen-containing species from the electrolyte, forming the O–Ni_2–N_6 structure, which then facilitates CO_2RR. O–Ni_2–N_6 with enhanced Ni–Ni interaction has a lower energy barrier for converting CO_2 to *COOH, which is considered the RDS (Fig. 13b). Compared with Ni–N_4 (0.18), the higher positive charge of 0.23 between the O–Ni_2–N_6 and the adsorbed *COOH intermediate indicates better activation of CO_2 on the dual-atom active site (Fig. 13c). Li et al. developed a supported Pd_2 DAC, which exhibited superior CO_2RR catalytic performance (98.2% FE_{CO} at − 0.85 V vs. RHE) and long-term stability [171]. The volcanic activity profile indicated that the superior CO_2RR performance of Pd_2 DAC could be attributed to the moderate adsorption strength of CO* on Pd_2 sites.

Besides the existence of two homometal sites, the heteronuclear metal atom catalysis would further enhance activity, stability, and selectivity by modulating the electronic structure of metal active centers [183, 184]. Chen et al. reported a DAC with a linked NiFe heteroatomic pair, significantly enhancing its electrocatalytic performance towards CO_2RR (94.5% FE for CO formation and 50.4 mA cm^{-2} at an overpotential of − 690 mV) and OER (10 mA cm^{-2} at an overpotential of 310 mV) [184]. The electronic structure analysis results revealed that Fe as the catalytic center shows a higher oxidation state due to its orbital coupling with Ni, which weakens binding strength with the intermediates and thus boosts the CO_2RR and OER electrocatalytic performance.

In addition to the linked metal sites, O-coordinating with dual-separated metal sites has also been reported [185–187]. For example, polyoxometalates ($Na_2WO_4{\cdot}2H_2O$ and $(NH_4)_6Mo_7O_{24}{\cdot}4H_2O$) consisting of metal oxide anion nanoclusters were selected to construct heteronuclear DAC (Fig. 13d) [185]. The O-coordinated W–Mo heterodimer anchored on N-doped graphene (W_1Mo_1–NG) was achieved with CVD treatment in the NH_3/Ar gas at 800 °C. Extended X-ray absorption fine structure (EXAFS) revealed the W–O–Mo–O–C configuration with strong covalent interactions (Fig. 13e, f). DFT results indicated that the electron delocalization of the O-coordinated W–Mo system afforded the desirable adsorption strength with hydrogen and improved HER kinetics. Figure 13g demonstrates that W_1Mo_1-NG displays the highest catalytic activity for the HER, which is evidenced by its almost zero onset potential in acidic electrolytes. The EXAFS fitting results, combined with DFT geometry optimization, suggest that the O-bridged W-Mo atoms are anchored in nitrogen-doped graphene (NG) vacancies, as depicted in Fig. 13h. The bridging oxygen in the W–O–Mo–O–C configuration as the active site shows optimal Gibbs free energy of hydrogen adsorption (ΔG_H) (Fig. 13i). The redistribution of the electronic structure due to the W–O–Mo–O–C configuration affords an improved electron environment for HER in pH-universal electrolysis.

Based on the different catalytic properties of DACs, their high activity can be attributed to the three mechanisms: (1) the electronic effect, in which the electronic structure of the metal center as the only adsorption site can be modulated by another metal center; (2) the synergistic

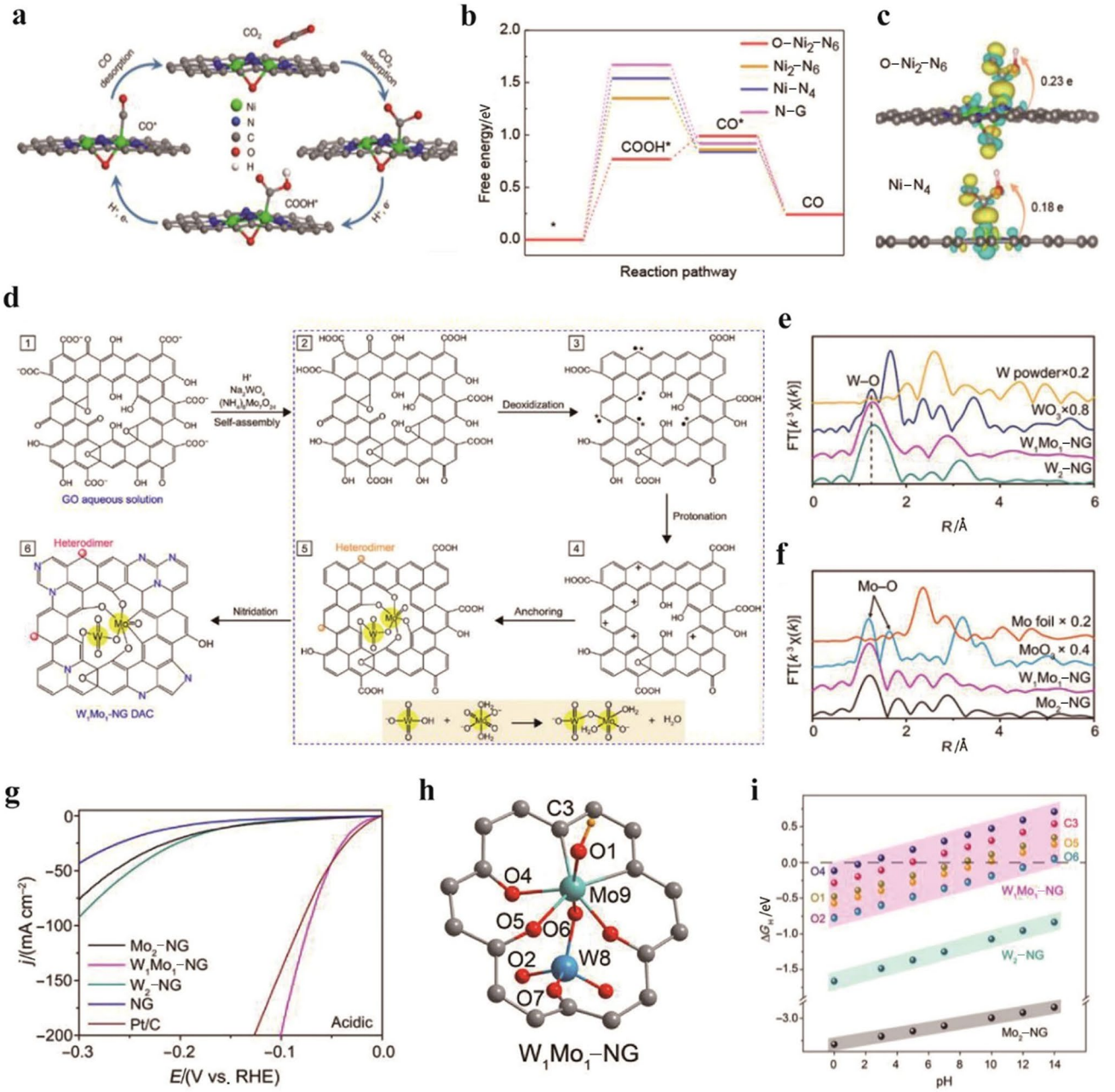

Fig. 13 **a** Proposed reaction pathways on O–Ni_2–N_6. **b** Calculated Gibbs free energy diagrams for CO_2 electroreduction to CO on various catalysts. **c** Electron density difference plot of the *COOH intermediate adsorption structure on O–Ni_2–N_6 and Ni–N_4 and the Bader charge analysis. Reproduced with permission from Ref. [188]. Copyright© 2021, American Chemical Society. **d** The proposed chemical mechanism of the synthetic procedure. **e**, **f** FT-EXAFS spectra of samples at Mo K-edge and W L_3-edge. **g** The polarization curves of samples in 0.5 mol L^{-1} H_2SO_4. **h** Optimized geometries and possible active sites for H adsorption on W_1Mo_1–NG. **i** ΔG_H diagrams of W_1Mo_1–NG, Mo_2–NG, and W_2–NG. Reproduced with permission from Ref. [185]. Copyright© 2020, American Association for the Advancement of Science

effect, in which two metal centers can separately act as adsorption sites for different intermediates; and (3) the adsorption effect, in which two metal centers, acting as the adsorption sites together, change the adsorption structures. Optimizing the adsorption structure of intermediates is one of the most effective ways to break the SRL and boost the catalytic activity. To achieve an in-depth insight into the synthetic and catalytic mechanisms of DACs, employing advanced controllable synthesis methods and atomic-scale characterization technologies is necessary and urgent.

3.2.4 Fully Exposed Cluster Catalysts (FECCs)

The concept of fully exposed cluster catalysts (FECCs) with almost full atom utilization efficiency was proposed based on the ratio of the exposed surface atoms [189]. Compared with SACs, FECCs with higher stable metal loading usually exhibit higher mass-specific activity, giving FECCs unique advantages in electrocatalysis [190–196]. Highly dispersed metal atoms on the support guarantee a high atomic utilization efficiency, providing rich sites for activating reactants and intermediates. Unlike conventional metal clusters or nanoparticle catalysts with many bulk atoms, the FECCs without bulk-phase metal atoms form a layered structure on support, significantly reducing the metal atoms' average coordination (Fig. 14a) [197]. Consequently, all atoms in these clusters are in the coordination-unsaturated state. In addition, the small contact angle with the support enhances the interaction between the metal atoms and the support. With full atomic utilization efficiency and unique atomic construction, FECCs have great potential in many catalytic reactions.

The concept of FECCs is put forward based on the successful fabrication of atomically-layered clusters or films [193, 195, 198]. Ma et al. synthesized a catalyst composed of layered gold (Au) clusters on molybdenum carbide (MoC) nanoparticles for thermocatalysis (Fig. 14b) [198]. Small epitaxial layered Au clusters had an average diameter of 1–2 nm and thickness of 2–4 atomic layers (< 1 nm). They found that the unique structure created rich Au-Mo interfacial sites to guarantee high CO coverage. Consequently, the reforming process involving the reaction of surface OH species formed on the Mo site with CO adsorbed on the adjacent Au surface was apt to proceed, leading to a low rate-determining step barrier toward the water–gas shift

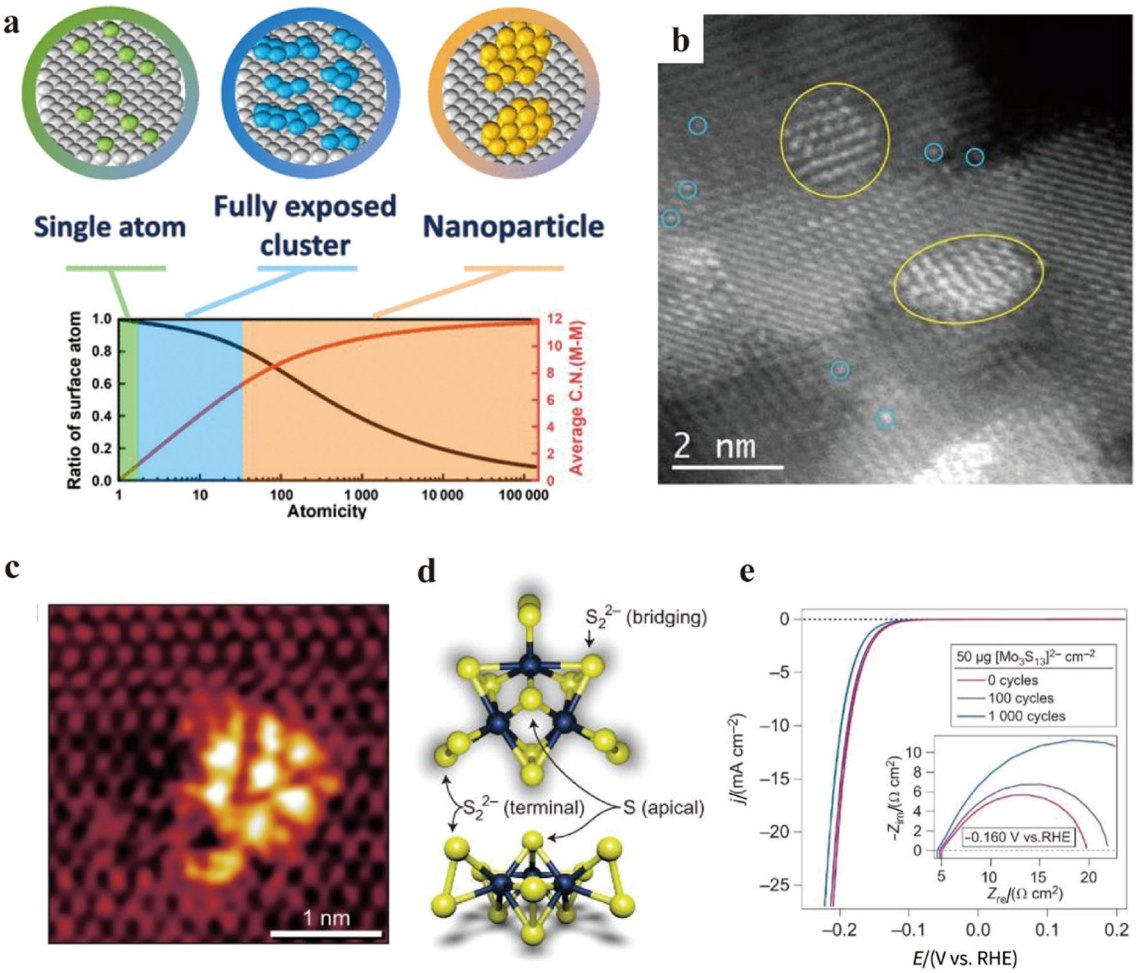

Fig. 14 **a** Schematic view and corresponding structure model of the SACs (left), FECCs (middle), and NPs (right). Reproduced with permission [197]. Copyright© 2021, American Chemical Society. **b** High-resolution high-angle annular dark-field (HAADF)-STEM images. Reproduced with permission [198]. Copyright© 2017, American Association for the Advancement of Science. **c** Atom-resolved STM image of a single $[Mo_3S_{13}]^{2-}$ cluster. **d** Model of a single $[Mo_3S_{13}]^{2-}$ cluster. **e** Accelerated stability test. Reproduced with permission [195]. Copyright© 2014, Springer

(WGS) reaction at low temperatures. The interfacial coordination nature was crucial in binding critical intermediates to active sites.

In addition, Besenbacher et al. report a sub-monolayer thiomolybdate $[Mo_3S_{13}]^{2-}$ nanocluster catalyst supported on highly orientated pyrolytic graphite (Fig. 14c–e) [195]. It has been reported that under-coordinated sulfur atoms at the edges of MoS_2 are highly active for HER, thus requiring MoS_2 with a high number of exposed edge sites. The STM image clearly shows highly dispersed individually-separated $[Mo_3S_{13}]^{2-}$ clusters on the surface (Fig. 14c). Three different types of sulfur ligands are all located intrinsically as edge sulfur atoms, enabling high HER activity and stability in acid (Fig. 14d, e). Wu et al. reported the use of a controllable thermal annealing method under a hydrogen atmosphere to prepare atomic-layered iridium supported on MXene ($Mo_2TiC_2T_x$) [86]. The successful morphology change from nanoparticles down to flattened atomic layers significantly enhanced the HER activity under alkaline conditions.

Strong chemical stabilization is usually required to synthesize atomically thin metallic layers. However, nearly all the metal atoms strongly bonded with chemical substrates or stabilizers, forming a core–shell or layer-by-layer structure, resulting in the shielding of most surface atoms and diminishing their real advantages. To explore the intrinsic properties of atomically-layered metal films, Wei et al. reported a self-stabilized and free-standing single-atom-layer PdCo film by using the angstrom-scaled interlayer space of layered minerals to eliminate the fundamental influences of substrate/stabilizer's coordination [199]. For the metallic single-atom-layer (SAL) structure, the absolute two-dimensional coordination environment displayed highly coordinated metallic bonds in two dimensions and dangling bonds in the *z*-direction. As a result, its valence/empty band at the Fermi level split into a lower-energy band in the *x*–*y* planes and a higher-energy band in the *z*-direction, which made PdCo metallic SAL stable and active for the ORR and electrolytic formic acid oxidation reaction (FAOR).

The successful preparation of atomically-layered clusters and the rapid development of advanced characterizations, particularly the HRSTEM (high-resolution TEM and STEM) imaging and synchrotron-radiated X-ray absorption spectroscopy (XAS), together enable building/establishing "structure–performance" relations. Thus, the concept of FECCs was formally proposed by Ma et al. in 2019 and then applied to the thermal catalysis field [189, 192, 197, 200]. It provides a novel platform to design effective and efficient catalysts for specific electrochemical processes, but related research as an emerging field is still in its infancy. Dang et al. introduced a type of single-cluster catalyst (Cu_7@[6]CPP) consisting of single-layered Cu clusters over a [6]cycloparaphenylene ([6]CPP) host [107]. Due to the neutral-cationic mixed valence state of the fully exposed central hexagonal-shaped Cu_7 cluster, Cu_7@[6]CPP showed a different CO reduction reaction path compared to that on a conventional Cu(111). Recently, Zhang et al. prepared N, S co-coordinated fully exposed Ni clusters anchored on carbon nanosheets [191]. The introduced S atoms contributed to the charge arrangement of multiple Ni centers and enhanced the adsorption of *COOH intermediates on Ni sites. As a result, the high CO current density (~347 mA cm^{-2} at − 0.8 V vs. RHE) and high selectivity towards CO with high faradayic efficiency (99% at an overpotential of 390 mV) were achieved. Xu et al. reported fully exposed atomically-layered Pt clusters (around 2 nm) supported on S-vacancy-rich MoS_{2-x} nanosheets [193]. The lattice fringe with an interplane spacing of 0.22 nm indicates that the atomic-layered Pt clusters are like active facets of Pt(111), which effectively enhance HER activity and durability in an acid electrolyte.

The FECCs with well-defined atomic structures are an ideal model catalyst to investigate the structure–property-performance relationship. However, the development of FECCs for electrocatalysis is still at an early stage in electrocatalysis applications. The controllable synthesis of FECCs with high structural uniformity is still tricky. In addition, structural reconstruction under working conditions frequently occurs, especially at high potentials.

4 Conclusion and Outlook

Significant progress has been achieved in the field of NCCs for electrocatalysis applications. This review provides a comprehensive summary of recently developed NCCs, encompassing synthetic methods and surface chemistry engineering for various electrocatalytic reactions (e.g., ORR, OER, CO_2RR, NRR and COR). We specifically emphasize surface and interface chemistry engineering for nanocluster fabrication and utilization, which includes (1) direct atomic engineering on nanoclusters (vacancy, heteroatom-doping, strain, multimetallic assembling, etc.) and (2) indirect modifications by SLCIs. The surface and interface coordination structures play a crucial role in determining their catalytic activity, selectivity, and stability in electrocatalysis applications. To elucidate their molecular-level structure and establish a structure–property-performance relationship, various types of NCCs, such as SNCs, HEAs, DACs, and FECCs, are presented and discussed. Importantly, this review emphasized how the unique geometric effects, electronic effects, and synergy effects determine the NCC's catalytic performance. However, the surface reconstruction and transformation of NCCs are prone to occur, especially in harsh operating conditions like electrochemical reactions due to the chemical and electrochemical leaching/dissolution. Therefore, advanced operando/in-situ characterization techniques are deemed necessary to unveil real-time structural

information and accurately clarify the catalytic mechanism. While the research of NCCs has demonstrated great potential in electrocatalysis, further advancement requires sustained efforts directed toward synthesis methodologies, advanced characterizations, and fundamental understandings of these materials.

4.1 Synthesis Methodologies

Advanced synthesis strategies have been developed for the controllable synthesis of metal clusters. Careful adjustment of synthesis parameters enables a controlled nucleation process, facilitating the management of the size and composition of metal nanoclusters on their supports. For instance, the host–guest strategy and ALD method are effective for precisely preparing atomic cluster catalysts. However, a critical restriction in developing high-performing NCCs is the lack of general methods to controllably synthesize atomic clusters with precise atom numbers on a large scale. To achieve uniform clusters with delicate structural or morphology control in terms of size, phase, shape, facets, and surface decoration, considerable effort and knowledge to understand the critical factors to obtain stable structures are required. Therefore, employing systematic experiments and theoretical calculations to determine the binding energy between metal–support and metal–metal would enable the design of stabler configurations of single-cluster catalysts.

4.2 Advanced Characterizations

Gaining in-depth insight into the synthetic and catalytic mechanisms of the local environment and identifying the exact cluster structures are crucially important yet challenging. Traditional heterogeneous NCCs often resemble a "black box", presenting significant challenges in characterizing and identifying active metal species. Characterizing the atomic configuration of NCCs is relatively more complicated than SACs due to their complex geometry and spatial assembling of multiple atoms. Atomic-resolved electron microscopes (e.g., HAADF-STEM) and spectroscopies (e.g., XAS) are two typical techniques for characterizing the atomic structure of NCCs. To assess their structure–activity/selectivity relationship, elucidating the actual cluster structure during the reaction process is vital, in addition to understanding the atomic coordination of pristine clusters. In recent years, the rapid advancement of in situ/operando characterization techniques has significantly transformed catalysis studies. Utilizing a combination of in situ/operando structural characterization techniques (such as STEM, X-ray Absorption Fine Structure (XAFS), and Infrared Spectroscopy (IR)) along with product analysis methods (including gas chromatography and mass spectrometry) will be a powerful approach to gain comprehensive insights into the dynamic structural changes of NCCs and to understand their real-time activation and deactivation mechanisms. To further unravel the complex NCCs, more advanced techniques, such as state-of-the-art in situ electron microscopies, should be considered. For example, atom probe tomography and atomic-resolution electron energy-loss spectroscopy are powerful in revealing cluster structures through chemical composition and three-dimensional imaging at the atomic level.

4.3 Fundamental Understanding

It is crucial to establish a foundational understanding of the dynamic evolution of surfaces under the catalyst operation conditions, as this profoundly influences the catalytic properties. The interface bonding of metal nanoclusters depends on the elemental composition, defects, ligands, and support. Recent advances in the synthesis and characterization of nanoclusters offer a conducive environment for understanding the catalytic mechanisms. Despite significant progress, several important issues remain unresolved, including atomic-level interface structures, electronic structure, structure–activity/selectivity relationships, and reaction pathways in NCCs for catalytic applications. For instance, new theories based on DFT calculations require urgent experimental verification. The novel interface structures need to consider the surface or interface elemental segregation reconstruction, lattice strain, and chemical diffusion, providing reliable inputs for theoretical calculations.

Acknowledgements This work was financially supported by the National Natural Science Foundation of China (22208331), the Natural Sciences and Engineering Research Council of Canada (NSERC), the Fonds de Recherche du Québec-Nature et Technologies (FRQNT), McGill University, Institut National de la Recherche Scientifique (INRS), and École de Technologie Supérieure (ÉTS). Dr. G. Zhang thanks for the support from the Marcelle-Gauvreau Engineering Research Chair program.

Declarations

Conflict of interest The authors declare that they have no known competing financial interests or personal relationships that could have appeared to influence the work reported in this paper. Shuhui Sun is an executive editor-in-chief for *Electrochemical Energy Reviews* and was not involved in the editorial review or the decision to publish this article. All authors declare that there are no competing interests.

References

1. Dong, H.M., Xue, M.G., Xiao, Y.J., et al.: Do carbon emissions impact the health of residents? Considering China's industrialization and urbanization. Sci. Total. Environ. **758**, 143688 (2021). https://doi.org/10.1016/j.scitotenv.2020.143688
2. Bai, H.W., Chen, D., Ma, Q.L., et al.: Atom doping engineering of transition metal phosphides for hydrogen evolution reactions.

Electrochem. Energy Rev. **5**, 24 (2022). https://doi.org/10.1007/s41918-022-00161-7
3. Niu, W.H., Yang, Y.: Graphitic carbon nitride for electrochemical energy conversion and storage. ACS Energy Lett. **3**, 2796–2815 (2018). https://doi.org/10.1021/acsenergylett.8b01594
4. Browne, M.P., Redondo, E., Pumera, M.: 3D printing for electrochemical energy applications. Chem. Rev. **120**, 2783–2810 (2020). https://doi.org/10.1021/acs.chemrev.9b00783
5. Wu, H.M., Feng, C.Q., Zhang, L., et al.: Non-noble metal electrocatalysts for the hydrogen evolution reaction in water electrolysis. Electrochem. Energy Rev. **4**, 473–507 (2021). https://doi.org/10.1007/s41918-020-00086-z
6. Gao, J.J., Tao, H.B., Liu, B.: Progress of nonprecious-metal-based electrocatalysts for oxygen evolution in acidic media. Adv. Mater. **33**, 2003786 (2021). https://doi.org/10.1002/adma.202003786
7. Li, F., Han, G.F., Baek, J.B.: Active site engineering in transition metal based electrocatalysts for green energy applications. Acc. Mater. Res. **2**, 147–158 (2021). https://doi.org/10.1021/accountsmr.0c00110
8. Guo, T., Li, L., Wang, Z.: Recent development and future perspectives of amorphous transition metal–based electrocatalysts for oxygen evolution reaction. Adv. Energy Mater. **12**, 2200827 (2022). https://doi.org/10.1002/aenm.202200827
9. Liu, L.C., Corma, A.: Metal catalysts for heterogeneous catalysis: from single atoms to nanoclusters and nanoparticles. Chem. Rev. **118**, 4981–5079 (2018). https://doi.org/10.1021/acs.chemrev.7b00776
10. Guo, Y., Mei, S., Yuan, K., et al.: Low-temperature CO_2 methanation over CeO_2-supported Ru single atoms, nanoclusters, and nanoparticles competitively tuned by strong metal–support interactions and H-spillover effect. ACS Catal. **8**, 6203–6215 (2018). https://doi.org/10.1021/acscatal.7b04469
11. Liu, D.B., He, Q., Ding, S.Q., et al.: Structural regulation and support coupling effect of single-atom catalysts for heterogeneous catalysis. Adv. Energy Mater. **10**, 2001482 (2020). https://doi.org/10.1002/aenm.202001482
12. Wu, T.Z., Han, M.Y., Xu, Z.J.: Size effects of electrocatalysts: more than a variation of surface area. ACS Nano **16**, 8531–8539 (2022). https://doi.org/10.1021/acsnano.2c04603
13. Zhou, M., Bao, S.J., Bard, A.J.: Probing size and substrate effects on the hydrogen evolution reaction by single isolated Pt atoms, atomic clusters, and nanoparticles. J. Am. Chem. Soc. **141**, 7327–7332 (2019). https://doi.org/10.1021/jacs.8b13366
14. Lopes, P.P., Li, D.G., Lv, H.F., et al.: Eliminating dissolution of platinum-based electrocatalysts at the atomic scale. Nat. Mater. **19**, 1207–1214 (2020). https://doi.org/10.1038/s41563-020-0735-3
15. Xia, C., Qiu, Y.R., Xia, Y., et al.: General synthesis of single-atom catalysts with high metal loading using graphene quantum dots. Nat. Chem. **13**, 887–894 (2021). https://doi.org/10.1038/s41557-021-00734-x
16. Wu, M.J., Zhang, G.X., Wang, W.C., et al.: Electronic metal–support interaction modulation of single-atom electrocatalysts for rechargeable zinc-air batteries. Small Meth. **6**, 2100947 (2022). https://doi.org/10.1002/smtd.202100947
17. Yang, M.X., Hou, Z.X., Zhang, X., et al.: Unveiling the origins of selective oxidation in single-atom catalysis via Co-N_4-C intensified radical and nonradical pathways. Environ. Sci. Technol. **56**, 11635–11645 (2022). https://doi.org/10.1021/acs.est.2c01261
18. Jin, X.X., Wang, R.Y., Zhang, L.X., et al.: Electron configuration modulation of nickel single atoms for elevated photocatalytic hydrogen evolution. Angew. Chem. **132**, 6894–6898 (2020). https://doi.org/10.1002/ange.201914565
19. Li, X.L., Xiang, Z.H.: Identifying the impact of the covalent-bonded carbon matrix to FeN_4 sites for acidic oxygen reduction. Nat. Commun. **13**, 57 (2022). https://doi.org/10.1038/s41467-021-27735-1
20. Dong, F., Wu, M.J., Chen, Z.S., et al.: Atomically dispersed transition metal–nitrogen–carbon bifunctional oxygen electrocatalysts for zinc-air batteries: recent advances and future perspectives. Nano-Micro Lett. **14**, 36 (2022). https://doi.org/10.1007/s40820-021-00768-3
21. Zhang, B.X., Chen, Y.P., Wang, J.M., et al.: Supported subnanometer clusters for electrocatalysis applications. Adv. Funct. Mater. **32**, 2202227 (2022). https://doi.org/10.1002/adfm.202202227
22. Ji, S.F., Chen, Y.J., Fu, Q., et al.: Confined pyrolysis within metal–organic frameworks to form uniform Ru_3 clusters for efficient oxidation of alcohols. J. Am. Chem. Soc. **139**, 9795–9798 (2017). https://doi.org/10.1021/jacs.7b05018
23. Kang, X., Li, Y.W., Zhu, M.Z., et al.: Atomically precise alloy nanoclusters: syntheses, structures, and properties. Chem. Soc. Rev. **49**, 6443–6514 (2020). https://doi.org/10.1039/c9cs00633h
24. Jin, R.C., Li, G., Sharma, S., et al.: Toward active-site tailoring in heterogeneous catalysis by atomically precise metal nanoclusters with crystallographic structures. Chem. Rev. **121**, 567–648 (2021). https://doi.org/10.1021/acs.chemrev.0c00495
25. Kwak, K., Lee, D.: Electrochemistry of atomically precise metal nanoclusters. Acc. Chem. Res. **52**, 12–22 (2019). https://doi.org/10.1021/acs.accounts.8b00379
26. Yao, C.H., Guo, N., Xi, S.B., et al.: Atomically-precise dopant-controlled single cluster catalysis for electrochemical nitrogen reduction. Nat. Commun. **11**, 4389 (2020). https://doi.org/10.1038/s41467-020-18080-w
27. Pérez-Ramírez, J., López, N.: Strategies to break linear scaling relationships. Nat. Catal. **2**, 971–976 (2019). https://doi.org/10.1038/s41929-019-0376-6
28. Jin, Y., Zhang, C., Dong, X.Y., et al.: Shell engineering to achieve modification and assembly of atomically-precise silver clusters. Chem. Soc. Rev. **50**, 2297–2319 (2021). https://doi.org/10.1039/d0cs01393e
29. Dong, C.Y., Li, Y.L., Cheng, D.Y., et al.: Supported metal clusters: fabrication and application in heterogeneous catalysis. ACS Catal. **10**, 11011–11045 (2020). https://doi.org/10.1021/acscatal.0c02818
30. Schubert, U.: Cluster-based inorganic–organic hybrid materials. Chem. Soc. Rev. **40**, 575–582 (2011). https://doi.org/10.1039/c0cs00009d
31. Yang, D., Babucci, M., Casey, W.H., et al.: The surface chemistry of metal oxide clusters: from metal-organic frameworks to minerals. ACS Cent. Sci. **6**, 1523–1533 (2020). https://doi.org/10.1021/acscentsci.0c00803
32. Guo, Y., Wang, M., Zhu, Q., et al.: Ensemble effect for single-atom, small cluster and nanoparticle catalysts. Nat. Catal. **5**, 766–776 (2022). https://doi.org/10.1038/s41929-022-00839-7
33. Rong, H.P., Ji, S.F., Zhang, J.T., et al.: Synthetic strategies of supported atomic clusters for heterogeneous catalysis. Nat. Commun. **11**, 5884 (2020). https://doi.org/10.1038/s41467-020-19571-6
34. Zhou, Y.Y., Xie, Z.Y., Jiang, J.X., et al.: Lattice-confined Ru clusters with high CO tolerance and activity for the hydrogen oxidation reaction. Nat. Catal. **3**, 454–462 (2020). https://doi.org/10.1038/s41929-020-0446-9
35. Feigerle, C.S., Bililign, S., Miller, J.C.: Nanochemistry: chemical reactions of iron and benzene within molecular clusters. J. Nanopart. Res. **2**, 147–155 (2000). https://doi.org/10.1023/a:1010034122603
36. Zhao, X., Wang, F.L., Kong, X.P., et al.: Subnanometric Cu clusters on atomically Fe-doped MoO_2 for furfural upgrading to aviation biofuels. Nat. Commun. **13**, 2591 (2022). https://doi.org/10.1038/s41467-022-30345-0

37. Zhang, B.H., Chen, J.S., Cao, Y.T., et al.: Ligand design in ligand-protected gold nanoclusters. Small **17**, 2004381 (2021). https://doi.org/10.1002/smll.202004381
38. Xue, Z.Q., Liu, K., Liu, Q.L., et al.: Missing-linker metal-organic frameworks for oxygen evolution reaction. Nat. Commun. **10**, 5048 (2019). https://doi.org/10.1038/s41467-019-13051-2
39. Yamamoto, K., Imaoka, T., Tanabe, M., et al.: New horizon of nanoparticle and cluster catalysis with dendrimers. Chem. Rev. **120**, 1397–1437 (2020). https://doi.org/10.1021/acs.chemrev.9b00188
40. Zhang, L., Si, R.T., Liu, H.S., et al.: Atomic layer deposited Pt-Ru dual-metal dimers and identifying their active sites for hydrogen evolution reaction. Nat. Commun. **10**, 4936 (2019). https://doi.org/10.1038/s41467-019-12887-y
41. Zhang, B.H., Zhao, G.Q., Zhang, B.X., et al.: Lattice-confined Ir clusters on Pd nanosheets with charge redistribution for the hydrogen oxidation reaction under alkaline conditions. Adv. Mater. **33**, 2105400 (2021). https://doi.org/10.1002/adma.202105400
42. Tian, S.B., Wang, B.X., Gong, W.B., et al.: Dual-atom Pt heterogeneous catalyst with excellent catalytic performances for the selective hydrogenation and epoxidation. Nat. Commun. **12**, 3181 (2021). https://doi.org/10.1038/s41467-021-23517-x
43. Tian, S.B., Fu, Q., Chen, W.X., et al.: Carbon nitride supported Fe_2 cluster catalysts with superior performance for alkene epoxidation. Nat. Commun. **9**, 2353 (2018). https://doi.org/10.1038/s41467-018-04845-x
44. Zhang, Z.Z., Ikeda, T., Murayama, H., et al.: Anchored palladium complex-generated clusters on zirconia: efficiency in reductive *N*-alkylation of amines with carbonyl compounds under hydrogen atmosphere. Chem. **17**, 2101243 (2022). https://doi.org/10.1002/asia.202101243
45. Liu, J.C., Xiao, H., Li, J.: Constructing high-loading single-atom/cluster catalysts via an electrochemical potential window strategy. J. Am. Chem. Soc. **142**, 3375–3383 (2020). https://doi.org/10.1021/jacs.9b06808
46. Shen, Y., Bo, X.K., Tian, Z.F., et al.: Fabrication of highly dispersed/active ultrafine Pd nanoparticle supported catalysts: a facile solvent-free in situ dispersion/reduction method. Green Chem. **19**, 2646–2652 (2017). https://doi.org/10.1039/c7gc00262a
47. Hou, C.C., Wang, H.F., Li, C.X., et al.: From metal-organic frameworks to single/dual-atom and cluster metal catalysts for energy applications. Energy Environ. Sci. **13**, 1658–1693 (2020). https://doi.org/10.1039/c9ee04040d
48. Karayilan, M., Brezinski, W.P., Clary, K.E., et al.: Catalytic metallopolymers from [2Fe-2S] clusters: artificial metalloenzymes for hydrogen production. Angew. Chem. Int. Ed. **58**, 7537–7550 (2019). https://doi.org/10.1002/anie.201813776
49. Li, J., Huang, H.L., Xue, W.J., et al.: Self-adaptive dual-metal-site pairs in metal-organic frameworks for selective CO_2 photoreduction to CH_4. Nat. Catal. **4**, 719–729 (2021). https://doi.org/10.1038/s41929-021-00665-3
50. Yao, K.L., Wang, H.B., Yang, X.T., et al.: Metal–organic framework derived dual-metal sites for electroreduction of carbon dioxide to HCOOH. Appl. Catal. B Environ. **311**, 121377 (2022). https://doi.org/10.1016/j.apcatb.2022.121377
51. Chen, S.R., Cui, M., Yin, Z.H., et al.: Single-atom and dual-atom electrocatalysts derived from metal organic frameworks: current progress and perspectives. Chemsuschem **14**, 73–93 (2021). https://doi.org/10.1002/cssc.202002098
52. Jiao, L., Jiang, H.L.: Metal-organic-framework-based single-atom catalysts for energy applications. Chem **5**, 786–804 (2019). https://doi.org/10.1016/j.chempr.2018.12.011
53. Wei, Y.S., Sun, L.M., Wang, M., et al.: Fabricating dual-atom iron catalysts for efficient oxygen evolution reaction: a heteroatom modulator approach. Angew. Chem. Int. Ed. **59**, 16013–16022 (2020). https://doi.org/10.1002/anie.202007221
54. Guo, X., Wan, X., Liu, Q.T., et al.: Phosphated IrMo bimetallic cluster for efficient hydrogen evolution reaction. eScience **2**, 304–310 (2022). https://doi.org/10.1016/j.esci.2022.04.002
55. Liu, X., Jia, S.F., Yang, M., et al.: Activation of subnanometric Pt on Cu-modified CeO_2 via redox-coupled atomic layer deposition for CO oxidation. Nat. Commun. **11**, 4240 (2020). https://doi.org/10.1038/s41467-020-18076-6
56. Zhang, B., Qin, Y.: Interface tailoring of heterogeneous catalysts by atomic layer deposition. ACS Catal. **8**, 10064–10081 (2018). https://doi.org/10.1021/acscatal.8b02659
57. Lu, Y.Y., Zhu, T.Y., van den Bergh, W., et al.: A high performing Zn-ion battery cathode enabled by in situ transformation of V_2O_5 atomic layers. Angew. Chem. **132**, 17152–17159 (2020). https://doi.org/10.1002/ange.202006171
58. Shen, T., Wang, S., Zhao, T.H., et al.: Recent advances of single-atom-alloy for energy electrocatalysis. Adv. Energy Mater. **12**, 2201823 (2022). https://doi.org/10.1002/aenm.202201823
59. Koy, M., Bellotti, P., Das, M., et al.: N-Heterocyclic carbenes as tunable ligands for catalytic metal surfaces. Nat. Catal. **4**, 352–363 (2021). https://doi.org/10.1038/s41929-021-00607-z
60. Du, Y.X., Sheng, H.T., Astruc, D., et al.: Atomically precise noble metal nanoclusters as efficient catalysts: a bridge between structure and properties. Chem. Rev. **120**, 526–622 (2020). https://doi.org/10.1021/acs.chemrev.8b00726
61. Yao, Y.G., Huang, Z.N., Li, T.Y., et al.: High-throughput, combinatorial synthesis of multimetallic nanoclusters. Proc. Natl. Acad. Sci. U.S.A. **117**, 6316–6322 (2020). https://doi.org/10.1073/pnas.1903721117
62. Shi, W.H., Liu, H.W., Li, Z.Z., et al.: High-entropy alloy stabilized and activated Pt clusters for highly efficient electrocatalysis. SusMat **2**, 186–196 (2022). https://doi.org/10.1002/sus2.56
63. Yao, Y.G., Dong, Q., Brozena, A., et al.: High-entropy nanoparticles: synthesis-structure-property relationships and data-driven discovery. Science **376**, eabn3103 (2022). https://doi.org/10.1126/science.abn3103
64. Yao, Y.G., Huang, Z.N., Xie, P.F., et al.: Carbothermal shock synthesis of high-entropy-alloy nanoparticles. Science **359**, 1489–1494 (2018). https://doi.org/10.1126/science.aan5412
65. Yao, Y.G., Huang, Z.N., Xie, P.F., et al.: High temperature shockwave stabilized single atoms. Nat. Nanotechnol. **14**, 851–857 (2019). https://doi.org/10.1038/s41565-019-0518-7
66. Yin, P., Luo, X., Ma, Y.F., et al.: Sulfur stabilizing metal nanoclusters on carbon at high temperatures. Nat. Commun. **12**, 3135 (2021). https://doi.org/10.1038/s41467-021-23426-z
67. Zhang, Z.L., Su, J., Matias, A.S., et al.: Enhanced and stabilized hydrogen production from methanol by ultrasmall Ni nanoclusters immobilized on defect-rich h-BN nanosheets. Proc. Natl. Acad. Sci. U.S.A. **117**, 29442–29452 (2020). https://doi.org/10.1073/pnas.2015897117
68. Reddy, K.P., Deshpande, P.A.: Density functional theory study of the immobilization and hindered surface migration of Pd_3 and Pd_4 nanoclusters over defect-ridden graphene: implications for heterogeneous catalysis. ACS Appl. Nano Mater. **4**, 9068–9079 (2021). https://doi.org/10.1021/acsanm.1c01661
69. Lin, Q.W., Zhang, J., Kong, D.B., et al.: Deactivating defects in graphenes with Al_2O_3 nanoclusters to produce long-life and high-rate sodium-ion batteries. Adv. Energy Mater. **9**, 1803078 (2019). https://doi.org/10.1002/aenm.201803078
70. Dong, Y., Wang, Y., Tian, Z.Q., et al.: Enhanced catalytic performance of Pt by coupling with carbon defects. Innov. **2**, 100161 (2021). https://doi.org/10.1016/j.xinn.2021.100161
71. Cheng, Q.Q., Hu, C.G., Wang, G.L., et al.: Carbon-defect-driven electroless deposition of Pt atomic clusters for highly

efficient hydrogen evolution. J. Am. Chem. Soc. **142**, 5594–5601 (2020). https://doi.org/10.1021/jacs.9b11524
72. Dai, Y.Q., Lu, P., Cao, Z.M., et al.: The physical chemistry and materials science behind sinter-resistant catalysts. Chem. Soc. Rev. **47**, 4314–4331 (2018). https://doi.org/10.1039/c7cs00650k
73. Cheng, Y., Wu, X., Veder, J.P., et al.: Tuning the electrochemical property of the ultrafine metal–oxide nanoclusters by iron phthalocyanine as efficient catalysts for energy storage and conversion. Energy Environ. Mater. **2**, 5–17 (2019). https://doi.org/10.1002/eem2.12029
74. Li, N., Shang, Y.X., Xu, R., et al.: Precise organization of metal and metal oxide nanoclusters into arbitrary patterns on DNA origami. J. Am. Chem. Soc. **141**, 17968–17972 (2019). https://doi.org/10.1021/jacs.9b09308
75. Ueda, M., Goo, Z.L., Minami, K., et al.: Structurally precise silver sulfide nanoclusters protected by rhodium(III) octahedra with aminothiolates. Angew. Chem. Int. Ed. **58**, 14673–14678 (2019). https://doi.org/10.1002/anie.201906425
76. Wang, X., Wang, X.L., Lv, J., et al.: 0D/1D heterostructure for efficient electrocatalytic CO_2-to-C_1 conversion by ultra-small cluster-based multi-metallic sulfide nanoparticles and MWCNTs. Chem. Eng. J. **422**, 130045 (2021). https://doi.org/10.1016/j.cej.2021.130045
77. Pan, X.N., Xi, B.J., Lu, H.B., et al.: Molybdenum oxynitride atomic nanoclusters bonded in nanosheets of N-doped carbon hierarchical microspheres for efficient sodium storage. Nano-Micro Lett. **14**, 163 (2022). https://doi.org/10.1007/s40820-022-00893-7
78. Chang, X.Q., Ma, Y.F., Yang, M., et al.: In-situ solid-state growth of N, S codoped carbon nanotubes encapsulating metal sulfides for high-efficient-stable sodium ion storage. Energy Storage Mater. **23**, 358–366 (2019). https://doi.org/10.1016/j.ensm.2019.04.039
79. Liu, Y.J., Xie, X.L., Zhu, G.X., et al.: Small sized Fe–Co sulfide nanoclusters anchored on carbon for oxygen evolution. J. Mater. Chem. A **7**, 15851–15861 (2019). https://doi.org/10.1039/c9ta03825f
80. Jing, W., Shen, H., Qin, R., et al.: Surface and interface coordination chemistry learned from model heterogeneous metal nanocatalysts: from atomically dispersed catalysts to atomically precise clusters. Chem. Rev. **123**, 5948–6002 (2023). https://doi.org/10.1021/acs.chemrev.2c00569
81. Mitchell, S., Pérez-Ramírez, J.: Atomically precise control in the design of low-nuclearity supported metal catalysts. Nat. Rev. Mater. **6**, 969–985 (2021). https://doi.org/10.1038/s41578-021-00360-6
82. Chen, S., Chen, Z.N., Fang, W.H., et al.: $Ag_{10}Ti_{28}$-oxo cluster containing single-atom silver sites: atomic structure and synergistic electronic properties. Angew. Chem. **131**, 11048–11051 (2019). https://doi.org/10.1002/ange.201904680
83. Chen, J.J., Li, X.N., Chen, Q., et al.: Neutral Au_1-doped cluster catalysts $AuTi_2O_{3-6}$ for CO oxidation by O_2. J. Am. Chem. Soc. **141**, 2027–2034 (2019). https://doi.org/10.1021/jacs.8b11118
84. Zhu, J.W., Lu, R.H., Shi, W.J., et al.: Epitaxially grown Ru clusters-nickel nitride heterostructure advances water electrolysis kinetics in alkaline and seawater media. Energy Environ. Sci. **6**, 12318 (2023). https://doi.org/10.1002/eem2.12318
85. Lv, L.Y., Tang, B., Ji, Q.Q., et al.: Highly exposed $NiFeO_x$ nanoclusters supported on boron doped carbon nanotubes for electrocatalytic oxygen evolution reaction. Chin. Chem. Lett. **34**, 107524 (2023). https://doi.org/10.1016/j.cclet.2022.05.038
86. Dai, L.X., Shen, Y.H., Chen, J.Z., et al.: MXene-supported, atomic-layered iridium catalysts created by nanoparticle redispersion for efficient alkaline hydrogen evolution. Small **18**, 2105226 (2022). https://doi.org/10.1002/smll.202105226
87. Lin, L., He, X.Y., Zhang, X.G., et al.: A nanocomposite of bismuth clusters and $Bi_2O_2CO_3$ sheets for highly efficient electrocatalytic reduction of CO_2 to formate. Angew. Chem. **135**, 2214959 (2023). https://doi.org/10.1002/ange.202214959
88. Gerber, I.C., Serp, P.: A theory/experience description of support effects in carbon-supported catalysts. Chem. Rev. **120**, 1250–1349 (2020). https://doi.org/10.1021/acs.chemrev.9b00209
89. van Deelen, T.V., Mejía, C.H., de Jong, K.D.: Control of metal-support interactions in heterogeneous catalysts to enhance activity and selectivity. Nat. Catal. **2**, 955–970 (2019). https://doi.org/10.1038/s41929-019-0364-x
90. Zhao, R.Y., Wang, Y.D., Ji, G.P., et al.: Partially nitrided Ni nanoclusters achieve energy-efficient electrocatalytic CO_2 reduction to CO at ultralow overpotential. Adv. Mater. **35**, 2205262 (2023). https://doi.org/10.1002/adma.202205262
91. Yan, X.C., Jia, Y., Wang, K., et al.: Controllable synthesis of Fe–N_4 species for acidic oxygen reduction. Carbon Energy **2**, 452–460 (2020). https://doi.org/10.1002/cey2.47
92. Zhang, G., Yang, X., Dubois, M., et al.: Non-PGM electrocatalysts for PEM fuel cells: effect of fluorination on the activity and stability of a highly active NC_Ar + NH_3 catalyst. Energy Environ. Sci. **12**, 3015–3037 (2019). https://doi.org/10.1039/c9ee00867e
93. Dodelet, J.P., Glibin, V., Zhang, G., et al.: Reply to the "Comment on 'Non-PGM electrocatalysts for PEM fuel cells: effect of fluorination on the activity and stability of a highly active NC_Ar + NH_3 catalyst'" by Xi Yin, Edward F. Holby and Piotr Zelenay. Energy Environ. Sci. **14**, 1034–1041 (2021). https://doi.org/10.1039/d0ee03431b
94. Wan, X., Liu, Q.T., Liu, J.Y., et al.: Iron atom–cluster interactions increase activity and improve durability in Fe–N–C fuel cells. Nat. Commun. **13**, 2963 (2022). https://doi.org/10.1038/s41467-022-30702-z
95. Ao, X., Zhang, W., Li, Z.S., et al.: Markedly enhanced oxygen reduction activity of single-atom Fe catalysts via integration with Fe nanoclusters. ACS Nano **13**, 11853–11862 (2019). https://doi.org/10.1021/acsnano.9b05913
96. Wei, X., Song, S., Cai, W., et al.: Tuning the spin state of Fe single atoms by Pd nanoclusters enables robust oxygen reduction with dissociative pathway. Chem **9**, 181–197 (2023). https://doi.org/10.1016/j.chempr.2022.10.001
97. Liu, H., Jiang, L.Z., Khan, J., et al.: Decorating single-atomic Mn sites with FeMn clusters to boost oxygen reduction reaction. Angew. Chem. **135**, 2214988 (2023). https://doi.org/10.1002/ange.202214988
98. Sun, F., Li, F., Tang, Q.: Spin state as a participator for demetalation durability and activity of Fe–N–C electrocatalysts. J. Phys. Chem. C **126**, 13168–13181 (2022). https://doi.org/10.1021/acs.jpcc.2c03518
99. Chen, Z.Y., Niu, H., Ding, J., et al.: Unraveling the origin of sulfur-doped Fe–N–C single-atom catalyst for enhanced oxygen reduction activity: effect of iron spin-state tuning. Angew. Chem. **133**, 25608–25614 (2021). https://doi.org/10.1002/ange.202110243
100. Xue, D.P., Yuan, P.F., Jiang, S., et al.: Altering the spin state of Fe–N–C through ligand field modulation of single-atom sites boosts the oxygen reduction reaction. Nano Energy **105**, 108020 (2023). https://doi.org/10.1016/j.nanoen.2022.108020
101. Gupta, S., Zhao, S., Wang, X.X., et al.: Quaternary FeCoNiMn-based nanocarbon electrocatalysts for bifunctional oxygen reduction and evolution: promotional role of Mn doping in stabilizing carbon. ACS Catal. **7**, 8386–8393 (2017). https://doi.org/10.1021/acscatal.7b02949
102. Li, J.Z., Chen, M.J., Cullen, D.A., et al.: Atomically dispersed manganese catalysts for oxygen reduction in proton-exchange

membrane fuel cells. Nat. Catal. **1**, 935–945 (2018). https://doi.org/10.1038/s41929-018-0164-8
103. Yan, Q.Q., Wu, D.X., Chu, S.Q., et al.: Reversing the charge transfer between platinum and sulfur-doped carbon support for electrocatalytic hydrogen evolution. Nat. Commun. **10**, 4977 (2019). https://doi.org/10.1038/s41467-019-12851-w
104. Gao, T.T., Tang, X.M., Li, X.Q., et al.: Understanding the atomic and defective interface effect on ruthenium clusters for the hydrogen evolution reaction. ACS Catal. **13**, 49–59 (2023). https://doi.org/10.1021/acscatal.2c04586
105. Zhao, Y.F., Kumar, P.V., Tan, X., et al.: Modulating Pt–O–Pt atomic clusters with isolated cobalt atoms for enhanced hydrogen evolution catalysis. Nat. Commun. **13**, 2430 (2022). https://doi.org/10.1038/s41467-022-30155-4
106. Liu, L.J., Wang, Z.Y., Wang, Z.Y., et al.: Mediating CO_2 electroreduction activity and selectivity over atomically precise copper clusters. Angew. Chem. **134**, 2205626 (2022). https://doi.org/10.1002/ange.202205626
107. Liu, Y.Q., Qiu, Z.Y., Zhao, X., et al.: Trapped copper in [6] cycloparaphenylene: a fully-exposed Cu_7 single cluster for highly active and selective CO electro-reduction. J. Mater. Chem. A **9**, 25922–25926 (2021). https://doi.org/10.1039/d1ta06688a
108. Gao, Z.H., Wei, K.C., Wu, T., et al.: A heteroleptic gold hydride nanocluster for efficient and selective electrocatalytic reduction of CO_2 to CO. J. Am. Chem. Soc. **144**, 5258–5262 (2022). https://doi.org/10.1021/jacs.2c00725
109. Tang, Q., Lee, Y.J., Li, D.Y., et al.: Lattice-hydride mechanism in electrocatalytic CO_2 reduction by structurally precise copper-hydride nanoclusters. J. Am. Chem. Soc. **139**, 9728–9736 (2017). https://doi.org/10.1021/jacs.7b05591
110. Sun, F., Tang, Q.: The ligand effect on the interface structures and electrocatalytic applications of atomically precise metal nanoclusters. Nanotechnology **32**, 352001 (2021). https://doi.org/10.1088/1361-6528/ac027c
111. Cao, Y.T., Guo, J.H., Shi, R., et al.: Evolution of thiolate-stabilized Ag nanoclusters from Ag-thiolate cluster intermediates. Nat. Commun. **9**, 2379 (2018). https://doi.org/10.1038/s41467-018-04837-x
112. Xu, G.T., Wu, L.L., Chang, X.Y., et al.: Solvent-induced cluster-to-cluster transformation of homoleptic gold(I) thiolates between catenane and ring-in-ring structures. Angew. Chem. Int. Ed. **58**, 16297–16306 (2019). https://doi.org/10.1002/anie.201909980
113. Pei, Y., Wang, P., Ma, Z.Y., et al.: Growth-rule-guided structural exploration of thiolate-protected gold nanoclusters. Acc. Chem. Res. **52**, 23–33 (2019). https://doi.org/10.1021/acs.accounts.8b00385
114. Zhang, M.M., Dong, X.Y., Wang, Y.J., et al.: Recent progress in functional atom-precise coinage metal clusters protected by alkynyl ligands. Coord. Chem. Rev. **453**, 214315 (2022). https://doi.org/10.1016/j.ccr.2021.214315
115. Hu, H.L., Lan, L.L., Zhang, T., et al.: Recent advances in polyoxometalate-based metal-alkynyl clusters. CrystEngComm **24**, 3317–3331 (2022). https://doi.org/10.1039/d2ce00190j
116. Zhang, M.M., Dong, X.Y., Wang, Z.Y., et al.: AIE triggers the circularly polarized luminescence of atomically precise enantiomeric copper(I) alkynyl clusters. Angew. Chem. **132**, 10138–10144 (2020). https://doi.org/10.1002/ange.201908909
117. Dhayal, R.S., van Zyl, W.E., Liu, C.W.: Copper hydride clusters in energy storage and conversion. Dalton Trans. **48**, 3531–3538 (2019). https://doi.org/10.1039/c8dt04639e
118. Liu, G., Poths, P., Zhang, X., et al.: CO_2 hydrogenation to formate and formic acid by bimetallic palladium–copper hydride clusters. J. Am. Chem. Soc. **142**, 7930–7936 (2020). https://doi.org/10.1021/jacs.0c01855
119. Shen, H., Xiang, S.J., Xu, Z., et al.: Superatomic Au_{13} clusters ligated by different N-heterocyclic carbenes and their ligand-dependent catalysis, photoluminescence, and proton sensitivity. Nano Res. **13**, 1908–1911 (2020). https://doi.org/10.1007/s12274-020-2685-0
120. Lei, Z., Endo, M., Ube, H., et al.: N-Heterocyclic carbene-based C-centered Au(I)-Ag(I) clusters with intense phosphorescence and organelle-selective translocation in cells. Nat. Commun. **13**, 4288 (2022). https://doi.org/10.1038/s41467-022-31891-3
121. Yuan, S.F., He, R.L., Han, X.S., et al.: Robust gold nanocluster protected with amidinates for electrocatalytic CO_2 reduction. Angew. Chem. Int. Ed. **60**, 14345–14349 (2021). https://doi.org/10.1002/anie.202103060
122. Tang, Q., Jiang, D.E.: Insights into the PhC≡C/Au interface. J. Phys. Chem. C **119**, 10804–10810 (2015). https://doi.org/10.1021/jp508883v
123. Hu, Q., Gao, K.R., Wang, X.D., et al.: Subnanometric Ru clusters with upshifted D band center improve performance for alkaline hydrogen evolution reaction. Nat. Commun. **13**, 3958 (2022). https://doi.org/10.1038/s41467-022-31660-2
124. Sun, M.H., Ji, J.P., Hu, M.Y., et al.: Overwhelming the performance of single atoms with atomic clusters for platinum-catalyzed hydrogen evolution. ACS Catal. **9**, 8213–8223 (2019). https://doi.org/10.1021/acscatal.9b02305
125. Wilcoxon, J.P., Abrams, B.L.: Synthesis, structure and properties of metal nanoclusters. Chem. Soc. Rev. **35**, 1162 (2006). https://doi.org/10.1039/b517312b
126. Kwon, G., Ferguson, G.A., Heard, C.J., et al.: Size-dependent subnanometer Pd cluster (Pd_4, Pd_6, and Pd_{17}) water oxidation electrocatalysis. ACS Nano **7**, 5808–5817 (2013). https://doi.org/10.1021/nn400772s
127. Wang, X.W., Qiu, S.Y., Feng, J.M., et al.: Confined Fe–Cu clusters as sub-nanometer reactors for efficiently regulating the electrochemical nitrogen reduction reaction. Adv. Mater. **32**, 2004382 (2020). https://doi.org/10.1002/adma.202004382
128. Wan, X.K., Wu, H.B., Guan, B.Y., et al.: Confining sub-nanometer Pt clusters in hollow mesoporous carbon spheres for boosting hydrogen evolution activity. Adv. Mater. **32**, 1901349 (2020). https://doi.org/10.1002/adma.201901349
129. Tan, Y.Y., Zhu, W.B., Zhang, Z.Y., et al.: Electronic tuning of confined sub-nanometer cobalt oxide clusters boosting oxygen catalysis and rechargeable Zn-air batteries. Nano Energy **83**, 105813 (2021). https://doi.org/10.1016/j.nanoen.2021.105813
130. Negreiros, F.R., Halder, A., Yin, C.R., et al.: Bimetallic Ag-Pt sub-nanometer supported clusters as highly efficient and robust oxidation catalysts. Angew. Chem. Int. Ed. **57**, 1209–1213 (2018). https://doi.org/10.1002/anie.201709784
131. Lu, Y.Z., Chen, W.: Sub-nanometre sized metal clusters: from synthetic challenges to the unique property discoveries. Chem. Soc. Rev. **41**, 3594 (2012). https://doi.org/10.1039/c2cs15325d
132. Ni, B., Shi, Y.A., Wang, X.: The sub-nanometer scale as a new focus in nanoscience. Adv. Mater. **30**, 1802031 (2018). https://doi.org/10.1002/adma.201802031
133. Ni, B., Wang, X.: Chemistry and properties at a sub-nanometer scale. Chem. Sci. **7**, 3978–3991 (2016). https://doi.org/10.1039/c6sc00432f
134. Zhang, H., Yang, Y., Liang, Y.X., et al.: Molecular stabilization of sub-nanometer Cu clusters for selective CO_2 electromethanation. Chemsuschem **15**, 2102010 (2022). https://doi.org/10.1002/cssc.202102010
135. Liu, S.S., Wang, M.F., Ji, H.Q., et al.: Altering the rate-determining step over cobalt single clusters leading to highly efficient ammonia synthesis. Natl. Sci. Rev. **8**, nwaa136 (2021). https://doi.org/10.1093/nsr/nwaa136
136. Luo, Y., Li, M.Y., Dai, Y.X., et al.: Transition metal-modified Co_4 clusters supported on graphdiyne as an effective nitrogen reduction reaction electrocatalyst. Inorg. Chem. **60**, 18251–18259 (2021). https://doi.org/10.1021/acs.inorgchem.1c02880

137. Yang, H.R., Luo, D., Gao, R., et al.: Reduction of N_2 to NH_3 by TiO_2-supported Ni cluster catalysts: a DFT study. Phys. Chem. Chem. Phys. **23**, 16707–16717 (2021). https://doi.org/10.1039/d1cp00859e
138. Luo, D., Ma, C.Y., Hou, J.F., et al.: Integrating nanoreactor with O-Nb-C heterointerface design and defects engineering toward high-efficiency and longevous sodium ion battery. Adv. Energy Mater. **12**, 2270071 (2022). https://doi.org/10.1002/aenm.202270071
139. Tian, H., Liang, J., Liu, J.: Nanoengineering carbon spheres as nanoreactors for sustainable energy applications. Adv. Mater. **31**, 1903886 (2019). https://doi.org/10.1002/adma.201903886
140. An, S.F., Zhang, G.H., Wang, T.W., et al.: High-density ultra-small clusters and single-atom Fe sites embedded in graphitic carbon nitride (g-C_3N_4) for highly efficient catalytic advanced oxidation processes. ACS Nano **12**, 9441–9450 (2018). https://doi.org/10.1021/acsnano.8b04693
141. Wang, N.N., Chen, X.D., Jin, J.T., et al.: Tungsten nitride atomic clusters embedded two-dimensional g-C_3N_4 as efficient electrocatalysts for oxygen reduction reaction. Carbon **169**, 82–91 (2020). https://doi.org/10.1016/j.carbon.2020.07.037
142. Patil, R., Liu, S.D., Yadav, A., et al.: Superstructures of zeolitic imidazolate frameworks to single- and multiatom sites for electrochemical energy conversion. Small **18**, 2203147 (2022). https://doi.org/10.1002/smll.202203147
143. Wu, Y.C., Wei, W., Yu, R.H., et al.: Anchoring sub-nanometer Pt clusters on crumpled paper-like MXene enables high hydrogen evolution mass activity. Adv. Funct. Mater. **32**, 2110910 (2022). https://doi.org/10.1002/adfm.202110910
144. Wu, M.J., Zhang, G.X., Qiao, J.L., et al.: Ultra-long life rechargeable zinc-air battery based on high-performance trimetallic nitride and NCNT hybrid bifunctional electrocatalysts. Nano Energy **61**, 86–95 (2019). https://doi.org/10.1016/j.nanoen.2019.04.031
145. Takahashi, M., Koizumi, H., Chun, W.J., et al.: Finely controlled multimetallic nanocluster catalysts for solvent-free aerobic oxidation of hydrocarbons. Sci. Adv. **3**, e1700101 (2017). https://doi.org/10.1126/sciadv.1700101
146. Zhang, B., Zheng, X.L., Voznyy, O., et al.: Homogeneously dispersed multimetal oxygen-evolving catalysts. Science **352**, 333–337 (2016). https://doi.org/10.1126/science.aaf1525
147. Wang, K., Huang, J., Chen, H., et al.: Recent progress in high entropy alloys for electrocatalysts. Electrochem. Energy Rev. **5**, 17 (2022). https://doi.org/10.1007/s41918-022-00144-8
148. Feng, G., Ning, F.H., Song, J., et al.: Sub-2 nm ultrasmall high-entropy alloy nanoparticles for extremely superior electrocatalytic hydrogen evolution. J. Am. Chem. Soc. **143**, 17117–17127 (2021). https://doi.org/10.1021/jacs.1c07643
149. Jin, Z.Y., Zhou, X.Y., Hu, Y.X., et al.: A fourteen-component high-entropy alloy@oxide bifunctional electrocatalyst with a record-low ΔE of 0.61 V for highly reversible Zn-air batteries. Chem. Sci. **13**, 12056–12064 (2022). https://doi.org/10.1039/d2sc04461g
150. Yu, L.L., Zeng, K.Z., Li, C.H., et al.: High-entropy alloy catalysts: from bulk to nano toward highly efficient carbon and nitrogen catalysis. Carbon Energy **4**, 731–761 (2022). https://doi.org/10.1002/cey2.228
151. Wu, D.S., Kusada, K., Yamamoto, T., et al.: Platinum-group-metal high-entropy-alloy nanoparticles. J. Am. Chem. Soc. **142**, 13833–13838 (2020). https://doi.org/10.1021/jacs.0c04807
152. Minamihara, H., Kusada, K., Wu, D.S., et al.: Continuous-flow reactor synthesis for homogeneous 1 nm-sized extremely small high-entropy alloy nanoparticles. J. Am. Chem. Soc. **144**, 11525–11529 (2022). https://doi.org/10.1021/jacs.2c02755
153. Yang, C.P., Ko, B.H., Hwang, S., et al.: Overcoming immiscibility toward bimetallic catalyst library. Sci. Adv. **6**, eaaz6844 (2020). https://doi.org/10.1126/sciadv.aaz6844
154. Cavin, J., Ahmadiparidari, A., Majidi, L., et al.: 2D high-entropy transition metal dichalcogenides for carbon dioxide electrocatalysis. Adv. Mater. **33**, 2100347 (2021). https://doi.org/10.1002/adma.202100347
155. Li, H.D., Han, Y., Zhao, H., et al.: Fast site-to-site electron transfer of high-entropy alloy nanocatalyst driving redox electrocatalysis. Nat. Commun. **11**, 5437 (2020). https://doi.org/10.1038/s41467-020-19277-9
156. Löffler, T., Savan, A., Meyer, H., et al.: Design of complex solid-solution electrocatalysts by correlating configuration, adsorption energy distribution patterns, and activity curves. Angew. Chem. Int. Ed. **59**, 5844–5850 (2020). https://doi.org/10.1002/anie.201914666
157. Zhang, D., Zhao, H., Wu, X.K., et al.: Multi-site electrocatalysts boost pH-universal nitrogen reduction by high-entropy alloys. Adv. Funct. Mater. **31**, 2006939 (2021). https://doi.org/10.1002/adfm.202006939
158. George, E.P., Raabe, D., Ritchie, R.O.: High-entropy alloys. Nat. Rev. Mater. **4**, 515–534 (2019). https://doi.org/10.1038/s41578-019-0121-4
159. Li, T.Y., Yao, Y.G., Huang, Z.N., et al.: Denary oxide nanoparticles as highly stable catalysts for methane combustion. Nat. Catal. **4**, 62–70 (2021). https://doi.org/10.1038/s41929-020-00554-1
160. Xu, H.D., Zhang, Z.H., Liu, J.X., et al.: Entropy-stabilized single-atom Pd catalysts via high-entropy fluorite oxide supports. Nat. Commun. **11**, 3908 (2020). https://doi.org/10.1038/s41467-020-17738-9
161. Song, B.A., Yang, Y., Rabbani, M., et al.: In situ oxidation studies of high-entropy alloy nanoparticles. ACS Nano **14**, 15131–15143 (2020). https://doi.org/10.1021/acsnano.0c05250
162. Li, R.Z., Wang, D.S.: Superiority of dual-atom catalysts in electrocatalysis: one step further than single-atom catalysts. Adv. Energy Mater. **12**, 2103564 (2022). https://doi.org/10.1002/aenm.202103564
163. Zhang, J., Huang, Q.A., Wang, J., et al.: Supported dual-atom catalysts: preparation, characterization, and potential applications. Chin. J. Catal. **41**, 783–798 (2020). https://doi.org/10.1016/S1872-2067(20)63536-7
164. Chen, Z.S., Zhang, G.X., Wen, Y.R., et al.: Atomically dispersed Fe–Co bimetallic catalysts for the promoted electroreduction of carbon dioxide. Nano-Micro Lett. **14**, 25 (2022). https://doi.org/10.1007/s40820-021-00746-9
165. Li, W.X., Guo, Z.H., Yang, J., et al.: Advanced strategies for stabilizing single-atom catalysts for energy storage and conversion. Electrochem. Energy Rev. **5**, 9 (2022). https://doi.org/10.1007/s41918-022-00169-z
166. Li, L.B., Yuan, K., Chen, Y.W.: Breaking the scaling relationship limit: from single-atom to dual-atom catalysts. Acc. Mater. Res. **3**, 584–596 (2022). https://doi.org/10.1021/accountsmr.1c00264
167. Zhou, W., Su, H., Cheng, W., et al.: Regulating the scaling relationship for high catalytic kinetics and selectivity of the oxygen reduction reaction. Nat. Commun. **13**, 6414 (2022). https://doi.org/10.1038/s41467-022-34169-w
168. Han, S.G., Ma, D.D., Zhu, Q.L.: Atomically structural regulations of carbon-based single-atom catalysts for electrochemical CO_2 reduction. Small Meth. **5**, 2100102 (2021). https://doi.org/10.1002/smtd.202100102
169. Leng, K.Y., Zhang, J.T., Wang, Y., et al.: Interfacial cladding engineering suppresses atomic thermal migration to fabricate well-defined dual-atom electrocatalysts. Adv. Funct. Mater. **32**, 2270227 (2022). https://doi.org/10.1002/adfm.202270227
170. Yin, C.Y., Li, Q., Zheng, J., et al.: Progress in regulating electronic structure strategies on Cu-based bimetallic catalysts for

CO_2 reduction reaction. Adv. Powder Mater. **1**, 100055 (2022). https://doi.org/10.1016/j.apmate.2022.100055
171. Zhang, N.Q., Zhang, X.X., Kang, Y.K., et al.: A supported Pd_2 dual-atom site catalyst for efficient electrochemical CO_2 reduction. Angew. Chem. **133**, 13500–13505 (2021). https://doi.org/10.1002/ange.202101559
172. Jia, Y.F., Li, F., Fan, K., et al.: Cu-based bimetallic electrocatalysts for CO_2 reduction. Adv. Powder Mater. **1**, 100012 (2022). https://doi.org/10.1016/j.apmate.2021.10.003
173. Wang, Y., Park, B.J., Paidi, V.K., et al.: Precisely constructing orbital coupling-modulated dual-atom Fe pair sites for synergistic CO_2 electroreduction. ACS Energy Lett. **7**, 640–649 (2022). https://doi.org/10.1021/acsenergylett.1c02446
174. Liang, Z., Song, L.P., Sun, M.Z., et al.: Tunable CO/H_2 ratios of electrochemical reduction of CO_2 through the Zn–Ln dual atomic catalysts. Sci. Adv. **7**, eabl4915 (2021). https://doi.org/10.1126/sciadv.abl4915
175. An, Q.Z., Jiang, J.J., Cheng, W.R., et al.: Recent advances in dual-atom site catalysts for efficient oxygen and carbon dioxide electrocatalysis. Small Methods **6**, 2200408 (2022). https://doi.org/10.1002/smtd.202200408
176. Hao, Q., Zhong, H.X., Wang, J.Z., et al.: Nickel dual-atom sites for electrochemical carbon dioxide reduction. Nat. Synth. **1**, 719–728 (2022). https://doi.org/10.1038/s44160-022-00138-w
177. Gao, D.F., Liu, T.F., Wang, G.X., et al.: Structure sensitivity in single-atom catalysis toward CO_2 electroreduction. ACS Energy Lett. **6**, 713–727 (2021). https://doi.org/10.1021/acsenergylett.0c02665
178. He, Q., Liu, D.B., Lee, J.H., et al.: Electrochemical conversion of CO_2 to syngas with controllable CO/H_2 ratios over Co and Ni single-atom catalysts. Angew. Chem. Int. Ed. **59**, 3033–3037 (2020). https://doi.org/10.1002/anie.201912719
179. Leverett, J., Tran-Phu, T., Yuwono, J.A., et al.: Tuning the coordination structure of Cu–N–C single atom catalysts for simultaneous electrochemical reduction of CO_2 and NO_3^- to urea. Adv. Energy Mater. **12**, 2201500 (2022). https://doi.org/10.1002/aenm.202201500
180. Chen, Y.Q., Zhang, J.R., Yang, L.J., et al.: Recent advances in non-precious metal–nitrogen–carbon single-site catalysts for CO_2 electroreduction reaction to CO. Electrochem. Energy Rev. **5**, 11 (2022). https://doi.org/10.1007/s41918-022-00156-4
181. Zhu, Z., Li, Z., Wang, J., et al.: Improving NiN_X and pyridinic N active sites with space-confined pyrolysis for effective CO_2 electroreduction. eScience **2**, 445–452 (2022). https://doi.org/10.1016/j.esci.2022.05.002
182. Gong, Y.N., Cao, C.Y., Shi, W.J., et al.: Modulating the electronic structures of dual-atom catalysts via coordination environment engineering for boosting CO_2 electroreduction. Angew. Chem. Int. Ed. **61**, 2215187 (2022). https://doi.org/10.1002/anie.202215187
183. Yao, D.Z., Tang, C., Zhi, X., et al.: Inter-metal interaction with a threshold effect in NiCu dual-atom catalysts for CO_2 electroreduction. Adv. Mater. **35**, 2209386 (2023). https://doi.org/10.1002/adma.202209386
184. Zeng, Z.P., Gan, L.Y., Yang, H.B., et al.: Orbital coupling of hetero-diatomic nickel–iron site for bifunctional electrocatalysis of CO_2 reduction and oxygen evolution. Nat. Commun. **12**, 4088 (2021). https://doi.org/10.1038/s41467-021-24052-5
185. Yang, Y., Qian, Y.M., Li, H.J., et al.: O-coordinated W–Mo dual-atom catalyst for pH-universal electrocatalytic hydrogen evolution. Sci. Adv. **6**, eaba6586 (2020). https://doi.org/10.1126/sciadv.aba6586
186. Wang, H., Liu, J.X., Allard, L.F., et al.: Surpassing the single-atom catalytic activity limit through paired Pt–O–Pt ensemble built from isolated Pt_1 atoms. Nat. Commun. **10**, 3808 (2019). https://doi.org/10.1038/s41467-019-11856-9
187. Fan, Z.Z., Luo, R.C., Zhang, Y.X., et al.: Oxygen-bridged indium–nickel atomic pair as dual-metal active sites enabling synergistic electrocatalytic CO_2 reduction. Angew. Chem. **135**, 2216326 (2023). https://doi.org/10.1002/ange.202216326
188. Ding, T., Liu, X.K., Tao, Z.N., et al.: Atomically precise dinuclear site active toward electrocatalytic CO_2 reduction. J. Am. Chem. Soc. **143**, 11317–11324 (2021). https://doi.org/10.1021/jacs.1c05754
189. Zhang, J.Y., Deng, Y.C., Cai, X.B., et al.: Tin-assisted fully exposed platinum clusters stabilized on defect-rich graphene for dehydrogenation reaction. ACS Catal. **9**, 5998–6005 (2019). https://doi.org/10.1021/acscatal.9b00601
190. Liu, D.W., Wang, B., Srinivas, K., et al.: Rich and uncovered FeN_x atom clusters anchored on nitrogen-doped graphene nanosheets for highly efficient and stable oxygen reduction reaction. J. Alloys Compd. **901**, 163763 (2022). https://doi.org/10.1016/j.jallcom.2022.163763
191. Hao, Q., Tang, Q., Zhong, H.X., et al.: Fully exposed nickel clusters with electron-rich centers for high-performance electrocatalytic CO_2 reduction to CO. Sci. Bull. **67**, 1477–1485 (2022). https://doi.org/10.1016/j.scib.2022.06.006
192. Jia, Z.M., Peng, M., Cai, X.B., et al.: Fully exposed platinum clusters on a nanodiamond/graphene hybrid for efficient low-temperature CO oxidation. ACS Catal. **12**, 9602–9610 (2022). https://doi.org/10.1021/acscatal.2c02769
193. Shi, F., Wu, W.Z., Chen, J.F., et al.: Atomic-layered Pt clusters on S-vacancy rich MoS_{2-x} with high electrocatalytic hydrogen evolution. Chem. Commun. **57**, 7011–7014 (2021). https://doi.org/10.1039/d1cc02304g
194. Zhang, Z.Y., Xu, X.F.: Mechanistic study on enhanced electrocatalytic nitrogen reduction reaction by Mo single clusters supported on MoS_2. ACS Appl. Mater. Interfaces **14**, 28900–28910 (2022). https://doi.org/10.1021/acsami.2c05649
195. Kibsgaard, J., Jaramillo, T.F., Besenbacher, F.: Building an appropriate active-site motif into a hydrogen-evolution catalyst with thiomolybdate $[Mo_3S_{13}]_2^-$ clusters. Nat. Chem. **6**, 248–253 (2014). https://doi.org/10.1038/nchem.1853
196. Ugartemendia, A., Mercero, J.M., de Cózar, A., et al.: Does the composition in PtGe clusters play any role in fighting CO poisoning? (2022). J. Chem. Phys. **156**, 209901 (2022). https://doi.org/10.1063/5.0098161
197. Peng, M., Dong, C.Y., Gao, R., et al.: Fully exposed cluster catalyst (FECC): toward rich surface sites and full atom utilization efficiency. ACS Cent. Sci. **7**, 262–273 (2021). https://doi.org/10.1021/acscentsci.0c01486
198. Yao, S.Y., Zhang, X., Zhou, W., et al.: Atomic-layered Au clusters on α-MoC as catalysts for the low-temperature water-gas shift reaction. Science **357**, 389–393 (2017). https://doi.org/10.1126/science.aah4321
199. Jiang, J.X., Ding, W., Li, W., et al.: Freestanding single-atom-layer Pd-based catalysts: oriented splitting of energy bands for unique stability and activity. Chem **6**, 431–447 (2020). https://doi.org/10.1016/j.chempr.2019.11.003
200. Dong, C.Y., Gao, Z.R., Li, Y.L., et al.: Fully exposed palladium cluster catalysts enable hydrogen production from nitrogen heterocycles. Nat. Catal. **5**, 485–493 (2022). https://doi.org/10.1038/s41929-022-00769-4

Mingjie Wu is a postdoctoral fellow at McGill University, Canada, and a Professor at the State Key Laboratory of New Textile Materials and Advanced Processing Technologies, Wuhan Textile University, China. He received his Ph.D degree from the Institut National de la Recherche Scientifique (INRS), Center for Energy, Materials, and Telecommunications, Canada (under the supervision of Prof. Shuhui Sun). His current research interests focus on ORR, OER, CO_2RR, and HER electrocatalysts for rechargeable metal-air batteries, metal-CO_2 batteries, PEM fuel cells, and water splitting.

Sasha Omanovic is a Professor of Chemical Engineering at McGill University. He obtained the "dipl.ing." (Chemical Engineering) and "Dr.Sc." (Chemistry) degrees at the University of Zagreb (Croatia), followed by a two-year post-doctoral position at Acadia University in Nova Scotia (Canada), where he studied the interaction of proteins with charged electrode surfaces. He joined McGill University in 2001, where he established the "Electrochemistry/Corrosion Laboratory". His research focuses on the development of electrodes for applications in the areas of wastewater treatment, energy conversion/storage, and on the investigation of corrosion processes and development of methods for corrosion protection, and functionalization of electrically-conducting surfaces for specific applications.

Shuhui Sun is a Full Professor at the Institut National de la Recherche Scientifique (INRS), center for Energy, Materials, and Telecommunications, Canada. He is a Fellow of the Canadian Academy of Engineering (CAE), and a Member of the Royal Society of Canada (RSC College). His current research interests focus on multifunctional nanomaterials for energy conversion and storage applications, including H_2 fuel cells, metal-ion (Li^+, Na^+, Zn^{2+}) batteries, lithium-metal batteries, metal-air batteries, solid-state batteries, etc. He is also interested in nanostructured photo- and electro-catalysts for H_2 production, CO_2 reduction, and water treatment.

Gaixia Zhang is a Marcelle-Gauvreau Engineering Research Chair Professor at École de Technologie Supérieure (ÉTS), University of Quebec, Montréal, Canada. She received her Ph.D. degree from Polytechnique Montréal, and then continued her research at Western University and INRS, Canada. Her research interests focus on advanced materials (catalysts, electrodes and electrolytes) for sustainable energy conversion and storage applications, including batteries, fuel cells, hydrogen production, and CO_2 reduction. She is also interested in interface and device engineering, as well as in-situ characterizations and theoretical simulations.